Benzyl [Methyl 5-acetamido-8-*O*-(5-acetamido-4,7,8,9-tetra-*O*-acetyl-3,5-dideoxy-D-*glycero*-α-D-*galacto*-2-nonulopyranosylono-1′,9-lactone)-4,7-di-*O*-acetyl-3,5-dideoxy-D-*glycero*-α-D-*galacto*-2-nonulopyranosylonate]-(2→3)-2,4,6-tri-*O*-benzoyl-β-D-galactopyranosyl-(1→3)-2-acetamido-4,6-di-*O*-benzoyl-2-deoxy-β-D-galactopyranosyl-(1→4)-{[methyl 5-acetamido-8-*O*-(5-acetamido-4,7,8,9-tetra-*O*-acetyl-3,5-dideoxy-D-*glycero*-α-D-*galacto*-2-nonulopyranosylono-1′,9-lactone)-4,7-di-*O*-acetyl-3,5-dideoxy-D-*glycero*-α-D-*galacto*-2-nonulopyranosylonate]-(2→3)}-2,6-di-*O*-benzoyl-β-D-galactopyranosyl-(1→4)-2,3,6-tri-*O*-benzyl-β-D-glucopyranosyl-(1→6)-2,3,4-tri-*O*-benzyl-β-D-glucopyranoside (43). To a mixture of **20** (140 mg, 0.0454 mmol) and **39** (66 mg, 0.0681 mmol) in CH_2Cl_2 (1.1 mL) was added 4 Å molecular sieves (AW-300) (210 mg) at room temperature. After stirring for 2 h and then cooling to 0 °C, TMSOTf (1.0 μL, 5.53 μmol) was added to the mixture. After stirring for 5 h at 0 °C as the reaction was monitored by TLC (PhMe/MeOH = 4:1), the reaction was quenched by saturated $NaHCO_3$ (aq) and filtered through a Celite pad, and the pad was washed with $CHCl_3$. The combined filtrate and washings were washed with brine, dried over Na_2SO_4, and concentrated. The resulting residue was purified by flash column chromatography using PhMe/MeOH (8:1) as the eluent to give **43** (140 mg, 80%): $[\alpha]_D = -5.0$ (*c* 2.0, $CHCl_3$); ^{1}H NMR (600 MHz, $CDCl_3$) δ 8.13−6.94 (m, 70 H, 14 Ph), 5.97 (br s, 1 H, H-4d), 5.78 (br d, 1 H, NH-d), 5.70 (d, 1 H, $J_{3,4}$ = 3.4 Hz, H-4e), 5.55 (dt, 1 H, $J_{3eq,4}$ = 4.8 Hz, $J_{3ax,4}$ = 13.0 Hz, $J_{4,5}$ = 10.3 Hz, H-4g), 5.52 (d, 1 H, $J_{5,NH}$ = 9.6 Hz, NH-b), 5.39−5.31 (m, 6 H, H-4b, 7b, 7g, and 3 NH), 5.28 (m, 1 H, H-2e), 5.24 (d, 1 H, $J_{1,2}$ = 8.9 Hz, H-1d), 5.20 (near t, 1 H, $J_{1,2}$ = 7.5 Hz, $J_{2,3}$ = 8.2 Hz, H-2c), 5.16 (m, 2 H, H-8b and 8g), 5.08 (m, 1 H, H-4f), 5.01 (dd, 1 H, $J_{6,7}$ = 1.7 Hz, $J_{7,8}$ = 10.3 Hz, H-7a), 4.95 (dt, 1 H, $J_{3eq,4}$ = 4.1 Hz, H-4a), 4.92−4.20 (14 d, 14 H, PhCH_2), 4.84 (dd, 1 H, H-7f), 4.67 (d, 1 H, $J_{1,2}$ = 7.5 Hz, H-1c), 4.63 (dt, 1 H, H-8f), 4.41 (d, 3 H, $J_{1,2}$ = 7.5 Hz, H-1e, 3e, and H-1h), 4.36 (d, 1 H, $J_{1,2}$ = 7.5 Hz, H-1h), 4.28−4.18 (m, 7 H, H-9′b, 9′g, 9f, 9a, 8a, 6b, and 5b), 4.13−3.98 (m, 8 H, H-5g, 5a, 3c, 4c, 5f, 9′a, 9b, and 9g), 3.91−3.35 (m, 11 H, Glc unit), 3.89 (br dd, 1 H, H-6g), 3.85 (br dd, 1 H, H-6f), 3.83 (br dd, 1 H, $J_{6,7}$ = 1.7 Hz, H-6a), 3.78 (s, 3 H, COOMe-a), 3.70 (br d, 1 H, H-9′f), 3.60 (m, 1 H, H-2d), 3.24 (s, 3 H, COOMe-f), 3.15 (m, 1 H, H-5h), 2.57 (dd, 1 H, J_{gem} = 13.0 Hz, $J_{3eq,4}$ = 4.8 Hz, H-3eq-b), 2.50 (dd, 1 H, J_{gem} = 13.0 Hz, $J_{3eq,4}$ = 4.8 Hz, H-3eq-g), 2.29 (br dd, 1 H, H-3eq-a), 2.11−1.78 (m, 55 H, 17 Ac, H-3ax-b, 3ax-a, 3ax-f, and 3eq-f), 1.63 (t, 1 H, J_{gem} = $J_{3ax,4}$ = 13.0 Hz, H-3ax-g); ^{13}C NMR (125 MHz, $CDCl_3$) δ 171.0, 170.7, 170.6, 170.6, 170.5, 170.5, 170.4, 170.3, 170.2, 169.8, 169.8, 169.7, 167.4, 167.3, 166.1, 166.0, 165.7, 165.7, 165.4, 164.7, 164.2, 138.8, 138.5, 138.5, 138.3, 138.2, 138.0, 137.5, 133.3, 133.2, 133.1, 133.0, 132.8, 132.8, 130.3, 129.9, 129.9, 129.7, 129.7, 129.6, 129.6, 129.5, 129.4, 129.3, 128.5, 128.3, 128.3, 128.2, 128.2, 128.2, 128.0, 128.0, 127.8, 127.7, 127.7, 127.6, 127.5, 127.4, 127.3, 103. 7, 102.6, 101.4, 100.0, 99.5, 99.0, 97.1, 96.0, 84.6, 82.8, 82.2, 81.5, 78.2, 76.2, 76.0, 75.6, 75.1, 75.0, 74.8, 74.8, 74.7, 74.3, 74.0, 73.3, 73.1, 72.5, 72.2, 72.0, 71.6, 71.4, 71.1, 70.8, 70.4, 69.9, 69.8, 69.5, 69.4, 69.4, 69.2, 69.0, 68.8, 68.6, 68.4, 68.4, 68.1, 67.3, 67.0, 66.7, 66.7, 63.4, 62.1, 62.0, 61.9, 54.6, 53.2, 52.4, 49.1, 48.9, 48.9, 38.7, 38.3, 35.7, 35.4, 29.6, 23.1, 23.0, 22.8, 20.8, 20.7, 20.7, 20.7, 20.6, 20.6, 20.3, 20.3; HRMS (ESI) *m/z* found $[M + 2Na]^{2+}$ 1967.1553, $C_{200}H_{217}N_5O_{75}$ calcd for $[M + 2Na]^{2+}$ 1967.1557.

[Methyl 5-acetamido-8-*O*-(5-acetamido-4,7,8,9-tetra-*O*-acetyl-3,5-dideoxy-D-*glycero*-α-D-*galacto*-2-nonulopyranosylono-1′,9-lactone)-4,7-di-*O*-acetyl-3,5-dideoxy-D-*glycero*-α-D-*galacto*-2-nonulopyranosylonate]-(2→3)-2,4,6-tri-*O*-benzoyl-β-D-galactopyranosyl-(1→3)-2-acetamido-4,6-di-*O*-benzoyl-2-deoxy-β-D-galactopyranosyl-(1→4)-{[methyl 5-acetamido-8-*O*-(5-acetamido-4,7,8,9-tetra-*O*-acetyl-3,5-dideoxy-D-*glycero*-α-D-*galacto*-2-nonulopyranosylono-1′,9-lactone)-4,7-di-*O*-acetyl-3,5-dideoxy-D-*glycero*-α-D-*galacto*-2-nonulopyranosylonate]-(2→3)}-2,6-di-*O*-benzoyl-β-D-galactopyranosyl-(1→4)-2-*O*-benzoyl-β-D-glucopyranosyl-(1→1)-(2*S*,3*R*,4*E*)-3-*O*-benzoyl-2-octadecanamido-4-octadecene-1,3-diol (44). To a solution of **40** (144 mg, 0.0351 mmol) in CH_2Cl_2 (4.0 mL) was added trifluoroacetic acid (2.0 mL) at 0 °C. After stirring for 1 h at 0 °C as the reaction was monitored by TLC (PhMe/MeOH = 4:1), the reaction mixture was diluted with $CHCl_3$. The organic layer was washed with ice-cooled saturated Na_2CO_3 (aq) (twice) and brine. After drying over Na_2SO_4 and being concentrated, the resulting residue was purified by flash column chromatography using $CHCl_3$/MeOH (25:1 to 10:1) to give **44** (131 mg, 97%): $[\alpha]_D = +4.7$ (*c* 0.5, $CHCl_3$); ^{1}H NMR (600 Hz, $CDCl_3$) δ 8.08−7.28 (m, 45 H, 9 Ph), 5.94 (br s, 1 H, H-4d), 5.86 (m, 1 H, $J_{4,5}$ = 15.1 Hz, $J_{5,6}$ = 7.5 Hz, $J_{5,6'}$ = 6.9 Hz, H-5i), 5.74 (d, 1 H, $J_{2,NH}$ = 9.6 Hz, NH-i), 5.70 (d, 1 H, $J_{3,4}$ = 3.4 Hz, H-4e), 5.57 (m, 1 H, H-4g), 5.54 (t, 1 H, $J_{2,3}$ = $J_{3,4}$ = 8.2 Hz, H-3i), 5.42 (dd, 1 H, $J_{3,4}$ = 8.2 Hz, $J_{4,5}$ = 15.1 Hz, H-4i), 5.38 (d, 1 H, $J_{5,NH}$ = 10.9 Hz, NH-f), 5.34 (m, 3 H, H-7b, 7g, and 2c), 5.28 (m, 1 H, H-2e), 5.20 (m, 2 H, H-8b and 8g), 5.16 (d, 1 H, $J_{1,2}$ = 8.2 Hz, H-1d), 5.10 (m, 2 H, H-4f and 2h), 5.00 (br dd, 1 H, H-7a), 4.92 (m, 1 H, H-4a), 4.86 (d, 2 H, H-7f and 3d), 4.77 (d, 1 H, $J_{1,2}$ = 7.5 Hz, H-1c), 4.72 (m, 1 H, H-6′c), 4.65 (br dt, 1 H, H-8f), 4.61 (m, 1 H, H-6′e), 4.45−4.39 (m, 7 H, H-1e, 3e, 1h, 4c, 5d, 5e, and 2i), 4.28−4.21 (m, 9 H, H-3c, 8a, 9′b, 9′g, 9′a, 9f, 5c, 6c, and 6e), 4.12 (q, 2 H, $J_{4,5}$ = 10.3 Hz, H-5g and 5b), 4.07−3.94 (m, 6 H, H-5f, 9b, 9g, 9a, 6d, and 6′d), 3.92−3.83 (m, 7 H, H-3h, 6g, 6b, 6f, 6a, 5a, and 1i), 3.77 (t, 1 H, $J_{4,5}$ = 9.6 Hz, H-4h), 3.76 (m, 4 H, COOMe-a and H-9′f), 3.64 (m, 1 H, H-2d), 3.50 (dd, 1 H, J_{gem} = 9.6 Hz, $J_{1',2}$ = 3.4 Hz, H-1′i), 3.24 (s, 3 H, COOMe-f), 3.16 (t, 1 H, J_{gem} = 10.9 Hz, H-6h), 3.05 (d, 1 H, $J_{4,5}$ = 9.6 Hz, H-5h), 2.91 (br dd, 1 H, J_{gem} = 10.9 Hz, H-6′h), 2.66 (dd, 1 H, 6h-OH), 2.59 (br dd, 1 H, H-3eq-b), 2.50 (dd, 1 H, $J_{3eq,4}$ = 5.4 Hz, J_{gem} = 12.3 Hz, H-3eq-g), 2.41 (br dd, 1 H, H-3eq-a), 2.11−1.81 (m, 58 H, 17 Ac, H-3eq-f, 3ax-f, 3ax-a, 3ax-b, 6i, 6′i, and NHCOCH_2), 1.63 (t, 1 H, J_{gem} = $J_{3ax,4}$ = 12.3 Hz, H-3ax-g), 1.43 (m, 1 H, NHCOCH_2), 1.26 (m, 52 H, 26 CH_2), 0.88 (t, 6 H, 2 Me); ^{13}C NMR (125 MHz, $CDCl_3$) δ 172.5, 171.1, 170.6, 170.5, 170.3, 170.1, 169.7, 169.6, 167.4, 167.2, 166.1, 166.0, 165.9, 165.7, 165.5, 165.4, 165.3, 164.7, 164.3, 164.1, 138.3, 133.2, 133.1, 133.0, 132.9, 132.7, 130.0, 129.9, 129.8, 129.7, 129.6, 129.5, 129.4, 129.4, 129.2, 129.1, 128.4, 128.3, 128.2, 124.6, 101.5, 101.3, 99.6, 99.4, 99.2, 98.9, 96.8, 95.8, 80.4, 75.8, 73.8, 73.6, 73.0, 72.7, 72.5, 72.3, 71.9, 71.5, 71.3, 71.7, 71.0, 70.5, 69.8, 69.7, 69.3, 69.3, 68.9, 68.7, 68.5, 68.2, 67.1, 66.9, 66.6, 66.6, 66.1, 64.0, 63.9, 62.3, 62.3, 62.2, 62.1, 62.0, 61.9, 61.9, 59.4, 54.7, 54.6, 54.6, 54.5, 54.5, 53.1, 52.2, 50.2, 49.1, 49.1, 48.9, 48.8, 48.7, 38.6, 38.2, 36.5, 35.4, 32.1, 31.7, 29.5, 29.5, 29.4, 29.4, 29.3, 29.2, 29.1, 28.7, 25.4, 22.9, 22.9, 22.7, 22.5, 20.7, 20.6, 20.6, 20.5, 20.5, 20.3, 20.2, 14.0; HRMS (ESI) *m/z* found $[M + 2Na]^{2+}$ 1948.7547, $C_{195}H_{242}N_6O_{74}$ calcd for $[M + 2Na]^{2+}$ 1948.7571.

2-(Trimethylsilyl)ethyl [Methyl 5-acetamido-8-*O*-(5-acetamido-4,7,8,9-tetra-*O*-acetyl-3,5-dideoxy-D-*glycero*-α-D-*galacto*-2-nonulopyranosylono-1′,9-lactone)-4,7-di-*O*-acetyl-3,5-dideoxy-D-*glycero*-α-D-*galacto*-2-nonulopyranosylonate]-(2→3)-2,4,6-tri-*O*-benzoyl-β-D-galactopyranosyl-(1→3)-2-acetamido-4,6-di-*O*-benzoyl-2-deoxy-β-D-galactopyranosyl-(1→4)-{[methyl 5-acetamido-8-*O*-(5-acetamido-4,7,8,9-tetra-*O*-acetyl-3,5-dideoxy-D-*glycero*-α-D-*galacto*-2-nonulopyranosylono-1′,9-lactone)-4,7-di-*O*-acetyl-3,5-dideoxy-D-*glycero*-α-D-*galacto*-2-nonulopyranosylonate]-(2→3)}-2,6-di-*O*-benzoyl-β-D-galactopyranosyl-(1→4)-2-*O*-benzoyl-β-D-glucopyranoside (45). To a solution of **42** (75 mg, 0.0215 mmol) in EtOH (2.1 mL) was added palladium hydroxide [20 wt % Pd (dry basis) on carbon, wet] (75 mg) at room temperature. After stirring for 33 h at 40 °C under a H_2 atmosphere as the reaction was monitored by TLC (PhMe/MeOH = 4:1), the mixture was filtered through a Celite pad and washed with $CHCl_3$. The combined filtrate and washings were concentrated. The resulting residue was purified by flash column chromatography using $CHCl_3$/MeOH (20:1 to 15:1) as the eluent to give **45** (63 mg, 90%): $[\alpha]_D = -2.3°$ (*c* 1.2, $CHCl_3$); ^{1}H NMR (500 MHz, $CDCl_3$) δ 8.10−7.26 (m, 40 H, 8 Ph), 5.93 (br s, 1 H, H-4d), 5.74 (br d, 1 H, NH-b), 5.70 (d, 1 H, $J_{3,4}$ = 3.6 Hz, H-4e), 5.55 (dt, 1 H, $J_{4,5}$ = 10.4 Hz, $J_{3eq,4}$ = 5.1 Hz, $J_{3ax,4}$ = 12.2 Hz, H-4g), 5.45 (d, 1 H, $J_{5',NH}$ = 10.0 Hz, NH-b), 5.34 (m, 7 H, H-4b, 2c, 2e, 7g, 7b, NH-g, and NH-f), 5.18 (d, 1 H, $J_{1,2}$ = 8.0 Hz, H-1d), 5.17 (m, 2 H, H-8b and 8g), 5.11 (t, 1 H, $J_{1,2}$

= 8.0 Hz, H-2h), 5.10 (m, 2 H, H-4f and NH-a), 5.01 (dd, 1 H, $J_{6,7}$ = 1.7 Hz, $J_{7,8}$ = 8.5 Hz, H-7a), 4.92 (m, 2 H, H-3d and 4a), 4.87 (dd, 1 H, $J_{6,7}$ = 1.7 Hz, $J_{7,8}$ = 9.5 Hz, H-7f), 4.77 (d, 1 H, $J_{1,2}$ = 8.0 Hz, H-1c), 4.71 (br dd, 1 H, H-6c), 4.63 (dt, 1 H, $J_{7,8}$ = 9.5 Hz, H-8f), 4.59 (m, 1 H, H-6e), 4.50 (d, 1 H, $J_{1,2}$ = 8.0 Hz, H-1h), 4.42 (m, 4 H, H-1e, 3e, 4c, and 6d), 4.29−4.19 (m, 11 H, H-5b, 8a, 3c, 6′e, 6b, 5e, 6′c, 9b, 9g, 9′f, and 9a), 4.12 (q, 1 H, $J_{4,5}$ = 10.4 Hz, $J_{5,6}$ = 10.2 Hz, H-5g), 4.06−3.98 (m, 5 H, H-5f, 9′a, 9′b, 9′g, and 6′d), 3.94−3.85 (m, 7 H, H-3h, 6g, 6f, 5a, 5c, 5d, and $OCH_2CH_2SiMe_3$), 3.81 (dd, 1 H, $J_{6,7}$ = 1.7 Hz, H-6a), 3.75 (m, 4 H, H-9f and COOMe-a), 3.69 (t, 1 H, $J_{3,4} = J_{4,5}$ = 8.7 Hz, H-4h), 3.63 (br q, 1 H, $J_{1,2}$ = 8.0 Hz, H-2d), 3.46 (m, 2 H, H-6h and $OCH_2CH_2SiMe_3$), 3.43 (m, 1 H, H-6′h), 3.30 (m, 1 H, H-5h), 3.24 (s, 3 H, COOMe-f), 2.57 (br dd, 1 H, H-3eq-b), 2.51 (dd, 1 H, J_{gem} = 12.2 Hz, $J_{3eq,4}$ = 5.1 Hz, H-3eq-g), 2.45 (m, 1 H, H-3eq-a), 2.11−1.70 (m, 55 H, 17 Ac, H-3ax-b, 3ax-a, 3eq-f, and 3ax-f), 1.64 (t, 1 H, $J_{gem} = J_{3ax,4}$ = 12.2 Hz, H-3ax-g), 0.82 (m, 2 H, $OCH_2CH_2SiMe_3$), 0.00 and −0.12 (2 s, 9 H, $OCH_2CH_2SiMe_3$); ^{13}C NMR (100 MHz, $CDCl_3$) δ 171.3, 170.7, 170.7, 170.6, 170.5, 170.4, 170.4, 170.4, 170.3, 169.9, 169.8, 169.8, 169.8, 169.7, 167.6, 167.3, 166.2, 166.1, 166.0, 165.6, 165.4, 165.1, 164.6, 164.5, 164.2, 133.5, 133.3, 133.3, 133.1, 133.0, 132.8, 130.3, 130.2, 129.9, 128.8, 129.7, 129.6, 129.6, 129.2, 128.6, 128.5, 128.4, 128.4, 128.2, 101.6, 100.5, 99.4, 99.2, 99.0, 97.1, 96.2, 81.2, 77.2, 75.8, 74.0, 73.8, 73.4, 73.2, 73.0, 72.8, 72.5, 72.1, 71.7, 71.4, 71.2, 70.6, 70.1, 69.9, 69.6, 69.4, 68.9, 68.8, 68.6, 68.5, 67.4, 67.3, 66.7, 64.0, 62.1, 62.0, 61.8, 60.6, 54.8, 53.2, 52.4, 49.3, 49.1, 49.1, 48.9, 38.6, 38.5, 38.3, 36.1, 35.6, 29.6, 23.1, 23.1, 23.0, 22.9, 20.8, 20.7, 20.7, 20.7, 20.6, 20.4, 20.3, 17.9, −1.1; HRMS (ESI) *m/z* found $[M + 2Na]^{2+}$ 1673.0130, $C_{157}H_{181}N_5O_{71}Si$ calcd for $[M + 2Na]^{2+}$ 1673.0130.

Acknowledgment. This work was financially supported by the Ministry of Education, Culture, Sports, Science, and Technology (MEXT) of Japan (Grant-in-Aid for Scientific Research to M.K., No. 17101007).

Supporting Information Available: Experimental data for compounds **8**−**10**, **12**, **13**, **17**−**19**, **23**, **24**, and **26**−**31**, and copies of ^1H and ^{13}C NMR spectra for all new compounds. This material is available free of charge via the Internet at http://pubs.acs.org.

JO8027888

Molecular Immunology 47 (2009) 606–613

Contents lists available at ScienceDirect

Molecular Immunology

journal homepage: www.elsevier.com/locate/molimm

Short communication

Efficient induction of human T-cell leukemia virus-1-specific CTL by chimeric particle without adjuvant as a prophylactic for adult T-cell leukemia

Tomohiro Kozako[a,b], Katsuhiko Fukada[c], Shinya Hirata[d], Yohann White[a], Michiko Harao[d], Yasuharu Nishimura[d], Youichiro Kino[c], Shinji Soeda[b], Hiroshi Shimeno[b], François Lemonnier[e], Shunro Sonoda[f], Naomichi Arima[a,*]

[a] Division of Hematology and Immunology, Center for Chronic Viral Diseases, Graduate School of Medical and Dental Sciences, Kagoshima University, Kagoshima, Japan
[b] Department of Biochemistry, Faculty of Pharmaceutical Sciences, Fukuoka University, Fukuoka, Japan
[c] The Chemo-Sero-Therapeutic Research Institute, Kumamoto, Japan
[d] Department of Immunogenetics, Graduate School of Medical Sciences, Kumamoto University, Kumamoto, Japan
[e] Unité d'Immunité Cellulaire Antivirale, Institut Pasteur, Paris, France
[f] International Island and Community Medicine, Graduate School of Medical and Dental Sciences, Kagoshima University, Kagoshima, Japan

ARTICLE INFO

Article history:
Received 25 June 2009
Received in revised form 1 September 2009
Accepted 3 September 2009
Available online 3 November 2009

Keywords:
Human T-cell leukemia virus-1
Adult T-cell leukemia/lymphoma
Cytotoxic T lymphocytes
Chimeric virus-like particle
Vaccine

ABSTRACT

Adult T-cell leukemia-lymphoma (ATL) is an aggressive peripheral T-cell neoplasm that develops after long-term infection with the human T-cell leukemia virus-1 (HTLV-1). HTLV-1-specific cytotoxic T lymphocytes (CTLs) play an important role in suppressing proliferation of HTLV-1-infected or transformed T-cells *in vitro*. Efficient induction of antigen-specific CTLs is important for immunologic suppression of oncogenesis, but has evaded strategies utilizing poorly immunogenic free synthetic peptides. In the present study, we examined the efficient induction of HTLV-1-specific CD8+ T-cell response by an HTLV-1/hepatitis B virus core (HBc) chimeric particle incorporating the HLA-A*0201-restricted HTLV-1 Tax-epitope. The immunization of HLA-A*0201-transgenic mice with the chimeric particle induced antigen-specific gamma-interferon reaction, whereas immunization with epitope peptide only induced no reaction as assessed by enzyme-linked immunospot assay. Immunization with the chimeric particle also induced HTLV-1-specific CD8+ T-cells in spleen and inguinal lymph nodes. Furthermore, upon exposure of dendritic cells from HLA-A*0201-transgenic mice to the chimeric particle, the expression of CD86, HLA-A02, TLR4 and MHC class II was increased. Additionally, our results show that HTLV-1-specific CD8+ T-cells can be induced by peptide with HTLV-1/HBc particle from ATL patient, but not by peptide only and these HTLV-1-specific CD8+ T-cells were able to lyse cells presenting the peptide. These results suggest that HTLV-1/HBc chimeric particle is capable of inducing strong cellular immune responses without adjuvants via effective maturation of dendritic cells and is potentially useful as an effective carrier for therapeutic vaccines in tumors, or in infectious diseases by substituting the epitope peptide.

1. Introduction

Adult T-cell leukemia-lymphoma (ATL) is an aggressive peripheral T-cell neoplasm, developing after long-term infection with HTLV-1 (Uchiyama, 1997). HTLV-1-specific CTLs play an important role in suppressing proliferation of HTLV-1-infected or transformed T-cells *in vitro* (Bangham, 2008; Jacobson et al., 1990). Additionally, we have previously reported the decreased frequency and function of HTLV-1 Tax-specific CD8+ T-cells in ATL patients, as characterized by insufficient cytolytic effector molecules, and have described the upregulation of the negative immuno-regulatory programmed death 1 (PD-1) marker on HTLV-1-specific CTLs from asymptomatic HTLV-1 carriers (ACs) and ATL patients (Kozako et al., 2006, 2009). Impaired host CTL function abrogates protection against accumulation of HTLV-1-transformed cells, and circumventing this hurdle may yield an effective immune strategy against leukemogenesis (Harashima et al., 2004; Yasunaga et al., 2001).

Antigen-specific CTL induction is an attractive immunotherapeutic strategy against hematologic malignancies and other cancers (Albert et al., 1998; Kawakami et al., 2008). The difficulty in inducing antigen-specific CTLs in individual patients vitiates a more widespread use of adoptive T-cell therapy. Whereas free synthetic peptides have proven to be relatively poor immunogens, viral-like particles (VLPs) have been consistently shown to induce strong antibody responses and CTLs, even without adjuvant (Grgacic and

* Corresponding author at: Division of Host Response, Center for Chronic Viral Diseases, Graduate School of Medical and Dental Sciences, Kagoshima University, 8-35-1 Sakuragaoka, Kagoshima 890-8544, Japan. Tel.: +81 99 275 5934; fax: +81 99 275 5947.
E-mail address: nao@m2.kufm.kagoshima-u.ac.jp (N. Arima).

0161-5890/$ – see front matter © 2009 Elsevier Ltd. All rights reserved.
doi:10.1016/j.molimm.2009.09.006

Anderson, 2006; Zhang et al., 2009). The hepatitis B core antigen (HBcAg), a potent immunogen eliciting strong humoral, T-helper and CTL responses and amenable to a variety of heterologous epitopes without adjuvant (Milich et al., 1987), is a potentially effective carrier protein for T-cell mediated vaccine development (Storni et al., 2002).

In the present study, we fused HTLV-1 Tax11–19 peptide, recognized by HLA-A*0201-restricted HTLV-1-specific CD8+ T-cells with high frequency (Kozako et al., 2006), to the HBcAg to synthesize an HTLV-1/HBc chimeric particle. We further examined the efficient induction of the HTLV-1-specific CD8+ T-cell response in HLA-A*0201-transgenic mice by the chimeric particle without adjuvant. This is the first study demonstrating the successful induction of HTLV-1-specific CD8+ T-cells in HLA-transgenic mice *in vivo*.

2. Materials and methods

2.1. Expression of recombinant chimeric particle in Pichia pastris

A synthetic DNA fragment, the HTLV-1 Tax sequence from amino acid positions 8–22 including the Tax11–19 epitope recognized by HLA-A*0201, was inserted into the HBc gene. The chimeric genes were PCR amplified by using pUC18 DNA vector (Takara, Japan) as a template. The sense primer 5′CGGGATCCACCATGGACATGGACCCGTATAAA3′ included a BamHI site (underlined) in the context of Kozac sequence. The antisense primer 5′GGAATTCTAACATTGAGATCCCCGAGA3′ included an EcoRI site (underlined). The purified PCR product was digested with the appropriate enzymes, and ligated to the BamHI and EcoRI treated *P. pastris* expression vector, pPIC3.5 (Fig. 1A, Invitrogen BV, Groningen, The Netherlands). The chimeric protein was expressed in *P. pastris* KM71.

P. pastris His+ transformants were grown in an L-tube in 5 ml of a rich standard medium [1% (w/v) yeast extract, 2% (w/v) peptone, 1.34% (w/v) yeast nitrogen base, 0.4 mg/l biotin and 100 mM potassium phosphate (pH 6.0)] containing 1% (w/v) glycerol (BMG), until OD600 reached 2–6. To begin the induction phase, cells were harvested by centrifugation and resuspended to an OD600 of 1 in rich standard medium containing 0.5% of methanol (BMM). Each subsequent day, 100% methanol was added to a final concentration of 0.5%. On the second day the yeast cells were harvested. Methanol-induced cultures were analyzed for HBcAg expression by using the ELISA. One transformant, isolated from the parental strain KM71, was selected for its high level of expression and was retained for large scale fermentation. The following large scale fermentation conditions were used: the dissolved oxygen concentration was maintained above 20% saturation; the pH was maintained at 5.5 throughout the fermentation process [with 28% (v/v) ammonium hydroxide], and the temperature was set at 30 °C using BMS-P I (Biot, Osaka).

The transformant was grown at 30 °C until OD600 reached 2–6 in a 5 L culture BMG medium. After exhausting the glycerol from the culture medium, 50% (w/v) glycerol, YPD and 100% methanol were supplied. Methanol supply was added to a final concentration of 0.5% in the culture medium over a 2-day period. The culture was harvested by centrifugation at 3000 × *g* for 10 min at 4 °C, and the cell pellet was recovered and stored at −80 °C until purification.

2.2. Preparation of the recombinant HTLV-1/HBc chimeric particle

Cell extracts were prepared by sonication at 0.02 g/ml in PBS containing 1 mM PMSF. After destruction, the cell suspension was centrifuged for 20 min at 10,000 rpm at 4 °C. The supernatant was filtered through a 0.45 μm membrane and then loaded onto anion-exchange DEAE-Toyopearl 650 mol/L chromatography column. HBcAg positive fractions detected by ELISA were examined by sedimentation through a sucrose step-wise gradient centrifugation. An aliquot (20 ml) of each sample was layered on top of a 40-ml step-wise sucrose gradient (30–60% [w/w]) in PBS and centrifuged at 30,000 rpm for 14 h at 4 °C with an RPST40T rotor (Hitachi, Japan). HBcAg positive fractions were dialyzed against a Tris–saline buffer on a 30,000 Da cutoff membrane and concentrated in an AMICON cell (Millipore S.A., St-Quentin-Yvelines, France). The products of HTLV-1/HBc chimeric particle were detected using methods previously described (Shiosaki et al., 1991). The monoclonal antibody used for the antigen analysis by ELISA and Western immunoblot was anti-HBc antibody (Miyanohara et al., 1986).

2.3. Animals

HLA-A2.1 (HHD) Tgm; H-2Db−/−β2m−/− double knockout mice introduced with human β2m-HLA-A2.1 (1 2)-H-2Db (three transmembrane cytoplasmic) (HHD) monochain construct gene were generated in the Department SIDA-Retrovirus, Unite d'Immunite Cellulaire Antivirale, Institut Pasteur, France (Pascolo et al., 1997).

2.4. Induction of HTLV-1-specific mouse CTLs

HLA-A*0201 (HHD) transgenic mice were immunized intradermally through the tail at days 0 and 14 with HTLV-1/HBc chimeric particle (20 μg), or Tax11–19 peptide (1 μg: LLFGYPVYV), assuming Tax11–19 epitope comprises one-twentieth of the HTLV-1/HBc protein. Simultaneous but uncombined immunization with HBc particle (20 μg) and peptide (1 μg) was also done. Cells (2×10^6 cells/well) from spleens and inguinal lymph nodes, harvested 7 days after the last immunization, were stimulated with Tax11–19 peptide *in vitro*. Then 6 days later, the frequency of cells producing gamma-interferon (IFN-γ) per 5, 10, 20×10^4 inguinal lymph node cells upon stimulation with syngenic bone marrow-derived dendritic cells (BM-DC) (1×10^4 cells/well) (Senju et al., 2003) (pulsed with or without each peptide) was assayed by enzyme-linked immunospot (ELISPOT) using the ELISPOT Set (Becton Dickinson, San Jose, CA) as previously described (Komori et al., 2006).

2.5. Maturation of dendritic cells

Murine immature dendritic cells (iDCs) were obtained from bone marrow (BM) precursors using a previously described method (Senju et al., 2003).

2.6. Flow cytometry

Phenotypic analysis using HTLV-1 Tax11–19 (LLFGYPVYV)/HLA-A*0201 tetramers was performed as described previously (Kozako et al., 2006, 2009). Matured DCs were immunostained with anti-mouse CD86 mAbs (clone: GL1; BD PharMingen, San Diego, CA), anti-mouse MHC class II mAbs (clone: NIMR-4; eBioscience, San Diego, CA), anti-mouse toll-like receptor (TLR4)/CD284 mAbs (clone: UT49; Medical and Biological Laboratories), and anti-HLA-A02 (clone: BB7.2; Santa Cruz Biotechnology, Santa Cruz, CA) mAbs as maturation markers by flow cytometry (FCM) on a FACScan (BD Biosciences). The data were expressed as mean fluorescence intensity (MFI) compared to unpulsed iDC controls.

2.7. Clinical samples

The subjects in this study included 6 ACs and 5 ATL patients, all of whom were recruited from Kagoshima University Hospital. Subjects were examined by standard serological testing for the

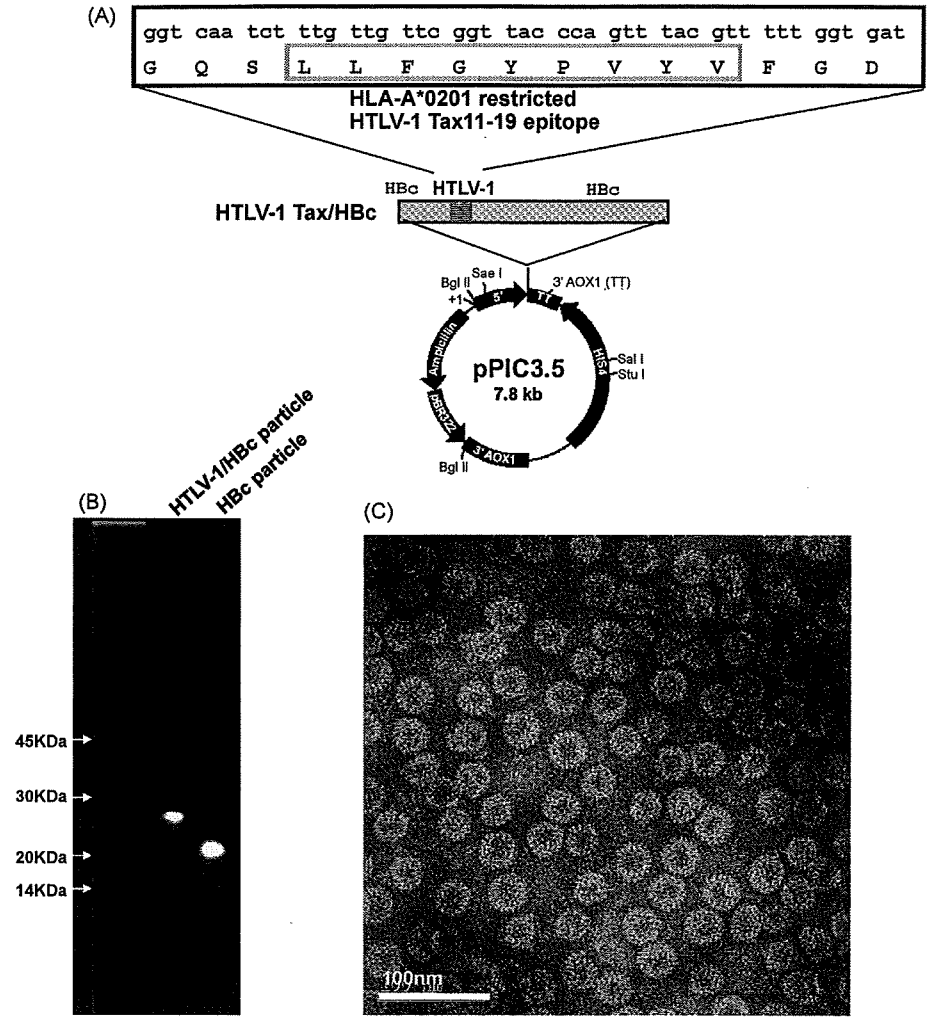

Fig. 1. Expression of recombinant HTLV-1/HBc chimeric particle. (A) The construction of HTLV-1/HBc chimeric protein. (B) Western blot profiles of the HTLV-1/HBc chimeric particle (left) and the HBc particle (right). The gene products were detected with anti-HBc antibody. (C) Electron micrograph of the HTLV-1/HBc chimeric particle. Original magnification × 100,000.

presence of HTLV-1 and by hematological/Southern blotting analysis for diagnosis of ATL. All subjects gave their written informed consent for participation in this study and to allow review of their medical records, and provided a sample of peripheral blood mononuclear cells (PBMCs) for human leukocyte antigen (HLA) typing and for the HLA tetramer assay (Kozako et al., 2006). The study protocol was reviewed and approved by the Medical Ethics Committee of Kagoshima University.

2.8. Preparation of PBMCs

PBMCs were obtained from peripheral blood by separation on Ficoll/Hypaque (Pharmacia, Uppsala, Sweden) density gradient centrifugation at 400 × *g* for 30 min, followed by washing 3 times with 1% FCS RPMI-1640 at 200 × *g* centrifugation for 10 min to remove residual platelets. The fresh PBMCs were used for tetramer assay and *ex vivo* expansion of anti-HTLV-1 CD8+ CTL. The remaining PBMCs were cryopreserved in liquid nitrogen until examination as described previously (Kozako et al., 2006).

2.9. Induction of HTLV-1 Tax-specific CD8+ T-cells from ACs and ATL patients

Aliquots of PBMCs (1×10^6 cells) were used for *in vitro* expansion of HTLV-1-specific CD8+ T-cell clones in cultures with each antigen in RPMI-1640 medium supplemented with the following reagents: 100 units/ml penicillin, 0.1 mg/ml streptomycin, 0.1 mM non-essential amino acids, 2 mM L-glutamine, 1 mM sodium pyruvate, 0.05 mM 2-mercaptoethanol, 50 units/ml of recombinant human interleukin-2, and 10% heat-inactivated fetal calf serum (RPMI-1640-CM). All culture conditions were the same as described elsewhere (Kozako et al., 2006). The cultured PBMCs were examined using the HTLV-1/HLA tetramer assay described below (Kozako et al., 2006).

2.10. Flow cytometric assay of cell mediated cytotoxicity

Cytotoxic activity of peptide-specific CTLs was evaluated using the T2-A2 cell line, *HLA-A*0201*-transfected, transporter associated with antigen processing-deficient (T × B) cell hybrid T2 cell line, which was maintained in RPMI-1640 supplemented with 10% FCS, 100 units/ml penicillin, 0.1 mg/ml streptomycin, and 2 mM L-glutamine, as targets by double staining (5 and 6)-carboxy fluorescein diacetate succinimidyl ester (WAKO, Japan) and Annexin V-PE-Cy5 (Medical and Biological Laboratories, Nagoya, Japan) (Aubry et al., 1999). Briefly, T2-A2 cells were incubated at 26 °C for 16 h, then incubated with/without HLA-A*0201-restricted HTLV-1 Tax peptide (LLFGYPVYV: 10 μM) or HLA-A*0201-restricted CMV pp65 peptide (NLVPMVATV: 10 μM) for 2 h at 26 °C followed by CFSE labeling. CFSE-labeled target cells were washed 3 times and

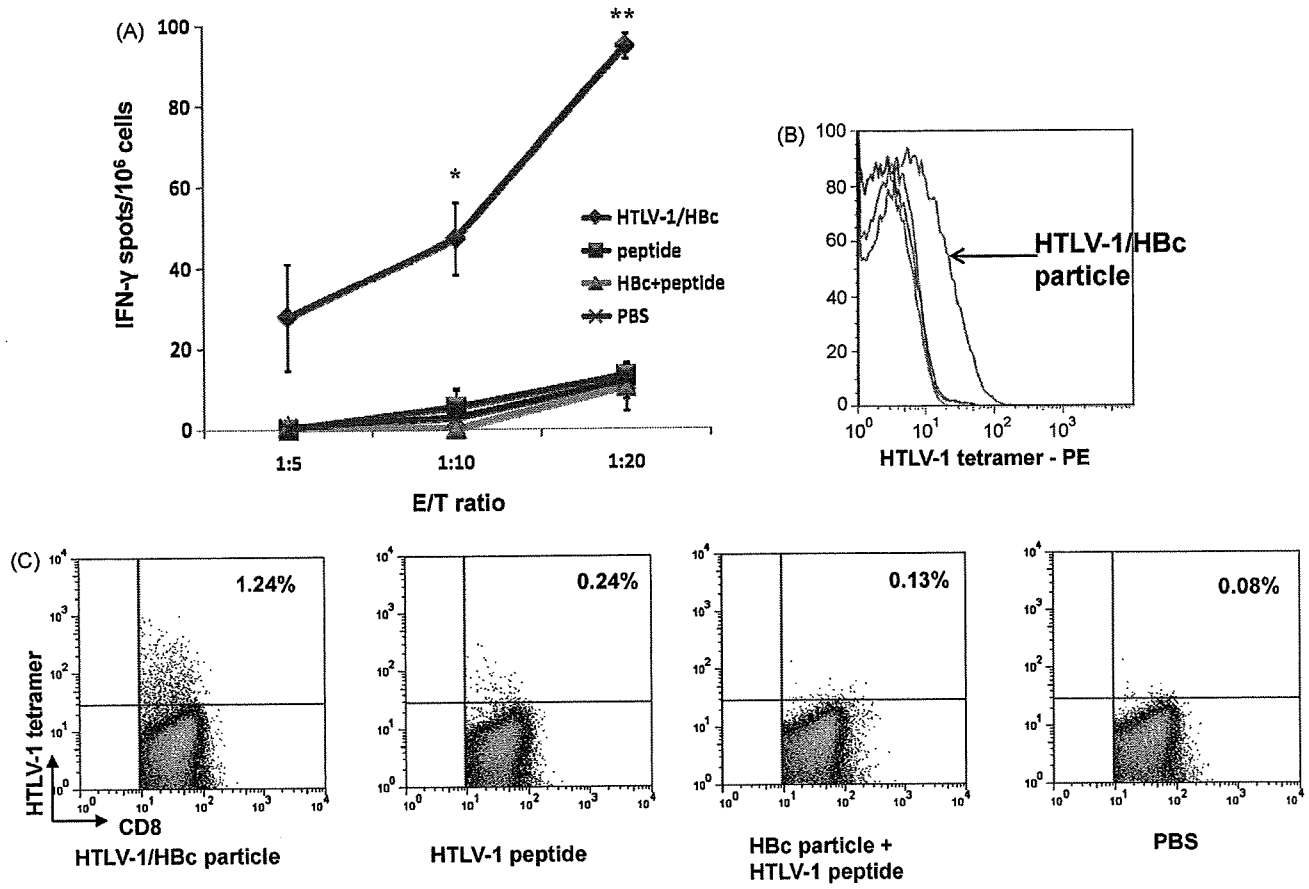

Fig. 2. Induction of cellular immunity by intradermal immunization with HTLV-1/HBc chimeric particle. (A) HLA-A*0201-transgenic mice were intradermally immunized twice with HTLV-1/HBc chimeric particle (20 μg), HTLV-1 peptide (1 μg: LLFGYPVYV), HTLV-1 peptide (1 μg) plus HBc particle (20 μg), or phosphate buffered saline (PBS) at days 0 and 14. Seven days after the last immunization, the spleens and inguinal lymph nodes were collected. The inguinal lymph node cells (2×10^6/well) were stimulated with Tax11–19 peptide *in vitro*. Then 6 days later, the frequency of cells producing IFN-γ per 5, 10, 20×10^4 inguinal lymph node cells upon stimulation with syngenic BM-DC (1×10^4/well), pulsed with or without each peptide, was determined by ELISPOT assay. IFN-γ spots are expressed as the number of peptide-loaded to peptide-unloaded target cells. $^*P < 0.05$, $^{**}P < 0.01$ vs PBS group. The experiments were performed in triplicates. Results represent means ± S.D. HTLV-1-specific CD8+ T-cell induction from spleen cells (B) and inguinal lymph node cells (C) by intradermal immunization with HTLV-1/HBc chimeric particle. Inguinal lymph node cells and spleen cells were harvested 7 days after the last immunization and stimulated with HTLV-1 peptide for 32 days. HTLV-1-specific CD8+ cells were analyzed by flow cytometry with anti-CD8-FITC and HTLV-1/HLA-A*0201 tetramer-PE. Numbers in the upper right quadrants represent the percentages of tetramer + CD8+ T-cells in CD8+ T lymphocytes.

seeded in a 96-well plate at a concentration of 1×10^4 cells/well. CTLs were added at 1:1, 5:1, 10:1 and 50:1 effector:target cell ratio and incubated for 4 h. All tests were performed in triplicate. Cytotoxicity (%) = [(ET − T0)/(100 − T0)] × 100; ET = Annexin V positive rate in the CFSE positive cells when target cells were co-cultured with effector cells. T0 = Annexin V positive rate in the CFSE positive cells when target cells were not co-cultured with effector cells.

2.11. Statistical analysis

Data obtained by FCM and ELISPOT assay were analyzed by two-tailed Student's *t*-test. A *P*-value < 0.05 was considered statistically significant. Statistical analyses were made using the StatView 5.0 software package (Abacus Concepts, Calabasas, CA).

3. Results

3.1. Expression of HTLV-1 Tax/HBc chimeric particle

We constructed an HTLV-1/HBc chimeric particle by inserting HTLV-1 Tax-epitope obtained from *P. pastris* His+ transformants. Protein was prepared by purification from yeast cell extracts as described previously (Shiosaki et al., 1991). HTLV-1/HBc chimeric protein expressed in *P. pastris* was collected in the fraction of 46–48% (w/w) sucrose. These results were nearly identical to the HBc protein (42–44%) (Miyanohara et al., 1986; Shiosaki et al., 1991). HTLV-1/HBc chimeric protein was collected in the high concentration fraction. The HTLV-1/HBc chimeric protein was 28 kDa, while the HBc protein was 21 kDa in Western blot analyses (Fig. 1B). As confirmed by electron microscopy, the chimeric particle from the yeast maintained the capacity to fold correctly, and spontaneously assembled into structured capsid particles with a diameter of 36 nm (Fig. 1C).

3.2. HTLV-1 Tax/HBc chimeric particle is immunogenic in the absence of adjuvant in vivo

The immune responses were investigated in HLA-A*0201-transgenic mice after intradermal immunization with HTLV-1 Tax/HBc chimeric particle. To determine the induction of humoral and cellular immunity, female mice were intradermally immunized twice at intervals of 14 days with HTLV-1 Tax/HBc chimeric particle, Tax peptide alone or HBc particle + Tax peptide. Seven days after the last immunization, inguinal lymph node cells from the mice immunized with these antigens were examined for their ability to induce IFN-γ-producing cells by ELISPOT assays. Immunization of HLA-A*0201-transgenic mice with the chimeric particle resulted in the efficient induction of IFN-γ-producing cells (Fig. 2A).

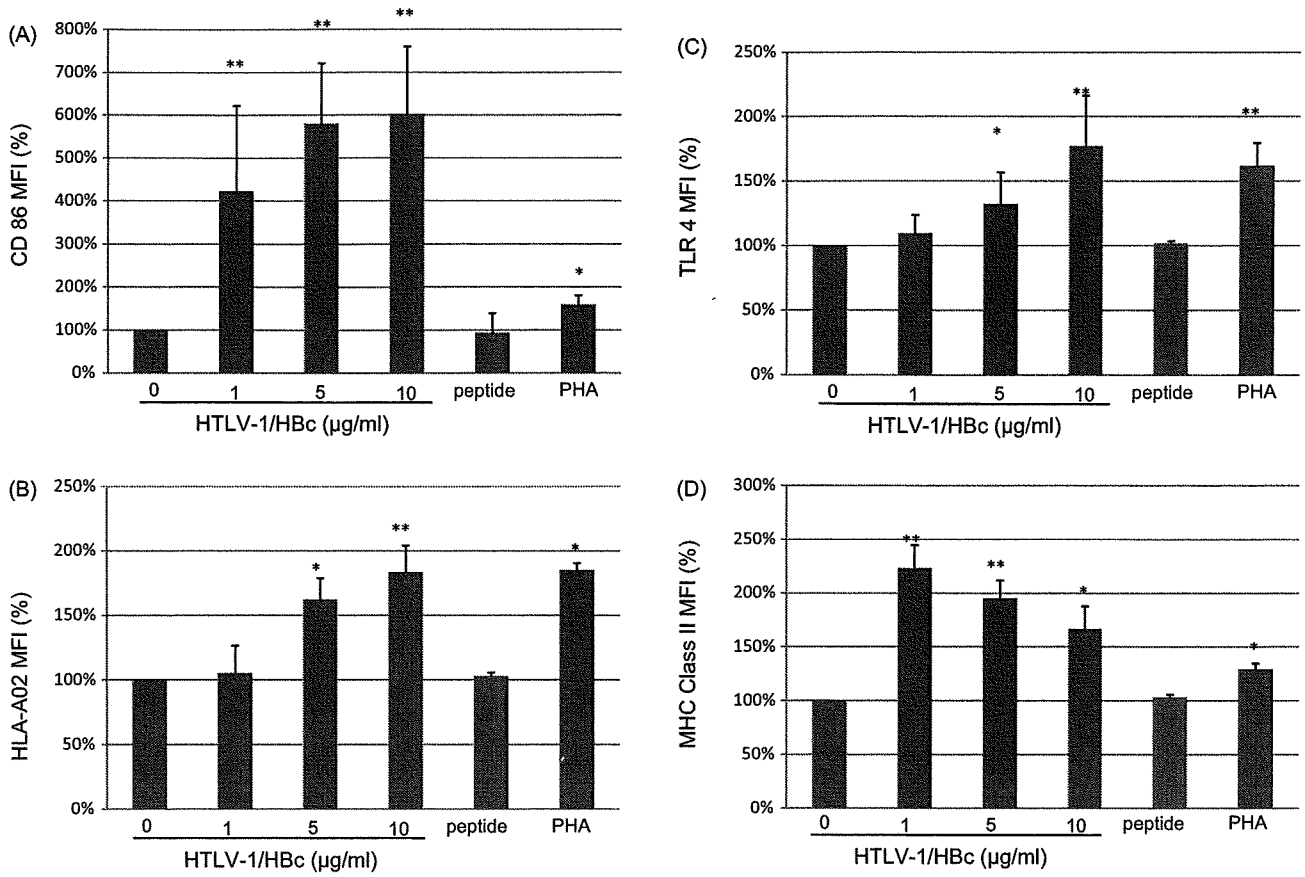

Fig. 3. Maturation of DCs induced by HTLV-1/HBc chimeric particle. Maturation of DCs induced by HTLV-1/HBc chimeric particle is illustrated by the expression of CD86 (A), HLA-A02 (B), TLR4 (C) and MHC class II (D) on the surface of DCs after incubation with antigens. The iDCs were incubated with the indicated concentrations of HTLV-1/HBc chimeric particle: 10 μg/ml of HTLV-1 peptide or 10 μg/ml of phytohemagglutinin (PHA) at 37 °C. Data are expressed as the mean fluorescence intensity (MFI) for each molecule compared to unpulsed (0 μg/ml) iDC controls. Results represent means ± S.D. for four independent experiments. $^{*}P<0.05$; $^{**}P<0.01$ vs unpulsed iDC controls.

This induction of IFN-γ-producing cells correlated well with effector cell increase, and was significantly higher than observed for either immunization with Tax peptide alone, or uncombined but simultaneous administration of HBc particle with Tax peptide.

We then measured HBc specific antibody levels in serum by ELISA. Mice immunized with HTLV-1 Tax/HBc chimeric particle or HBc particle had high levels of anti-HBc IgG in their sera, while mice immunized with Tax peptide had no anti-HBc IgG. IgG concentrations for HTLV-1 Tax/HBc chimeric particle and HBc particle displayed sigmoid kinetics (data not shown).

3.3. HTLV-1 Tax/HBc chimeric particle induces HTLV-1-specific CD8+ T-cells

To examine HTLV-1 Tax-specific CD8+ cell induction, spleen cells and inguinal lymph node cells from mice immunized with HTLV-1 Tax/HBc chimeric particle were stimulated with Tax peptide *in vitro*. HTLV-1 Tax-specific CD8+ cells from spleen and inguinal lymph nodes were detected by tetramer assay. The induction of HTLV-1 Tax-specific CD8+ cells from spleen (Fig. 2B) and inguinal lymph nodes (Fig. 2C) was observed after immunization with HTLV-1 Tax/HBc chimeric particle.

3.4. Maturation of DCs through uptake of chimeric particle

Dendritic cell maturation is associated with increased expression of several cell surface markers, including the co-stimulatory molecules CD86 and MHC class II. To determine whether phenotypic maturation of DCs was mediated by chimeric particle uptake, iDCs were incubated with HTLV-1/HBc chimeric particle for 48 h, and the expression of surface molecules was measured by FCM. Upon exposure of these DCs to the chimeric particle, the expression of CD86 and HLA-A02 was increased in a dose-dependent manner (Fig. 3A and B). As a positive control, PHA-pulsed DCs displayed a marked increase in maturation markers as well, while HTLV-1 epitope peptide did not upregulate these surface markers. HTLV-1/HBc chimeric particle also upregulated the expression of TLR4 in a dose-dependent manner compared to unpulsed control iDCs (Fig. 3C). In addition, the chimeric particle resulted in a marked increase in MHC class II expression at 1 μg/ml, but which trended downwards at concentrations equal to or greater than 5 μg/ml chimeric particle (Fig. 3D).

3.5. Induction of HTLV-1 Tax-specific CD8+ T-cells from ATL patients and ACs and cytotoxic activity of induced CTL

PBMCs from ACs or ATL patients were cultured with or without 20 μM of Tax11–19 peptide (LLFGYPVYV) or 0.5 μM of HTLV-1/HBc chimeric particle. An increase in the proportion of Tax11–19 tetramer positive cells was evident for AC cells exposed to peptide or chimeric particle (5 of 6, representative data shown in Fig. 4A), with similar levels of induction. In contrast, we observed no increase in the proportion of Tax11–19 positive cells for ATL patient cells ($n=5$ patients) exposed to either Tax11–19 peptide or chimeric particle alone, although a combination of both peptide and chimera elicited modest increases (in 2 of 2 ATL patient sam-

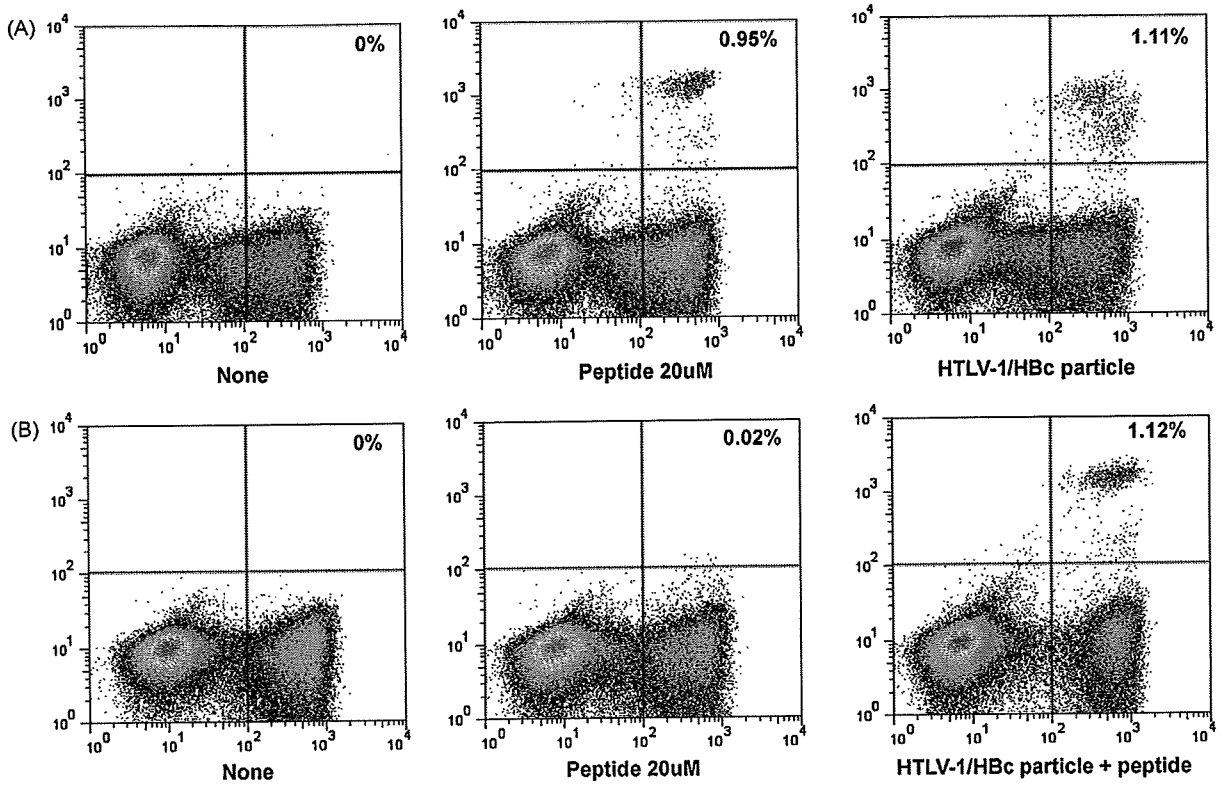

Fig. 4. Induction of HTLV-1 Tax-specific CD8+ T-cells from ACs and ATL patients. Freshly isolated PBMCs from ACs (A) and ATL patients (B) were cultured without peptide (left), with peptide (middle), with HTLV-1/HBc particle (right in A) or with peptide + HTLV-1/HBc particle (right in B). Numbers in the upper right quadrants represent the percentages of tetramer + CD8+ T-cells in T lymphocytes.

ples, representative data shown in Fig. 4B). Induction of tetramer positive cells was highly variable among asymptomatic carriers, with increases sometimes evident even in the absence of peptide or chimera; conversely, peptide or chimera sometimes resulted in no induction (data not shown).

Furthermore, these HTLV-1-specific CD8+ cells induced apoptosis of HTLV-1 epitope peptide-pulsed T2-A2 cells (Fig. 5). The T-cells efficiently lysed T2-A2 target cells pulsed with the peptide expressing Annexin V, whereas only low background lysis was observed in the absence of Tax peptide, or for CMV peptide-loaded T2-A2 cells. These results demonstrated that the HTLV-1/HBc chimeric particle-induced CTL response was MHC class I restricted, specifically lysing cells presenting the appropriate peptide.

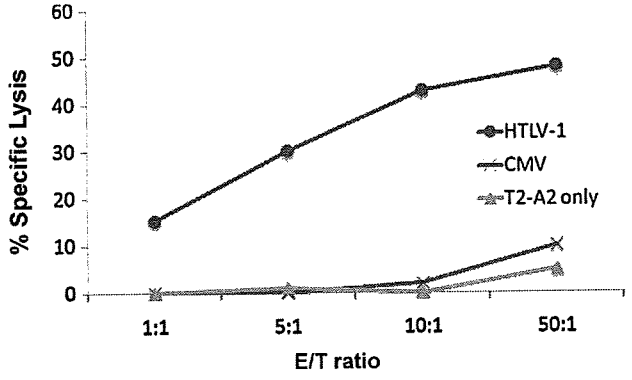

Fig. 5. Cytotoxic activity of induced HTLV-1-specific CD8+ T-cells. Using HTLV-1 peptide and CMV peptide-loaded and unpulsed T2-A2 cells as target cells, specific cytotoxic activity was evaluated by flow cytometric assay of cell mediated cytotoxicity. All tests were performed in triplicate and at effector:target ratios of 1:1, 5:1, 10:1 and 50:1.

4. Discussion

Viral-like particles have been demonstrated to prime CTL and antibody responses *in vivo* (Qian et al., 2006; Storni et al., 2002). HBc particles with a diameter of 33 nm have been synthesized by the yeast glyceraldehyde-3-phosphate dehydrogenase promoter and terminator, *Escherichia coli* K802d, *E. coli* BL21 cell and the yeast strain AH22 (Imamura et al., 1987; Shiosaki et al., 1991; Storni et al., 2002; Zhang et al., 2007). Here, we obtained HTLV-1/HBc chimeric particle inserting HTLV-1 epitope from *P. pastris* His+ transformants. As confirmed by electron microscopy, the chimeric product maintained the capacity to correctly fold and self-assemble into structured capsid particles with a diameter of 36 nm (Fig. 1B). These results indicate that the HTLV-1/HBc chimeric particle, using a different expression system, behaved as anticipated.

Immunization of HLA-A*0201-transgenic mice with the chimeric particle resulted in the efficient induction of IFN-γ-producing cells. This induction of IFN-γ-producing cells correlated well with effector cell increase, and was significantly higher than observed for either immunization with Tax peptide alone, or uncombined but simultaneous administration of HBc particle with Tax peptide. These results may be attributable to an adjuvant effect on the immune response by HBc capsids. It is known, for example, that T helper epitopes in the HBc protein augment CTL development and enhance CD8+ memory T-cell survival. Others have reported on the efficient processing of lymphocytic choriomeningitis virus-derived p33/HBc chimera via cross-presentation, although only weak CTL responses were induced in C57BL/6 mice (Storni et al., 2002). Thus, while VLPs alone are inefficient at inducing CTL responses, they become very potent vaccines when combined with antigen presenting cell (APC) activating substances like anti-CD40 mAbs or nonmethylated CG

motif-rich DNA (CpGs). We demonstrated the efficient induction of IFN-γ-producing cells and HTLV-1-specific CD8+ cells from spleens and inguinal lymph nodes by the HTLV-1/HBc chimeric particle in HLA-A*0201-transgenic mice. These results may be due to the efficient processing of the HTLV-1/HBc chimeric particle by DCs for MHC class I associated presentation in this human mouse model.

Dendritic cell maturation is intricately involved in the processing and presentation of antigens to T-cells through increased expression of MHC class I, MHC class II, and CD86 co-stimulatory molecules (Banchereau and Steinman, 1998). Exposure of bone marrow-derived iDCs to the HTLV-1/HBc chimeric particle increased the expression of CD86 and HLA-A02 in a dose-dependent manner, in contradistinction to peptide only stimulation. Expression levels of co-stimulatory molecules and TLR4 in the chimeric particle-pulsed DCs were significantly greater than for PHA-pulsed DCs. These results suggest that the uptake of HTLV-1/HBc chimeric particle by iDCs supports the phenotypic and functional maturation of DCs without adjuvant, likely via TLR4 signaling. It is known that VLPs can enhance activation and maturation of DCs (Da Silva et al., 2007), but there has been no report on whether HBc particles increase co-stimulatory molecule expression in HLA-A*0201-transgenic mice. The present study therefore demonstrates that the HTLV-1/HBc chimeric particle is able to activate APCs, such as macrophages and DCs, which in turn have the ability to cross-present VLPs and other particulate antigens.

HTLV-1 carriers showing insufficient T-cell responses to HTLV-1, despite and especially in the presence of high viral loads, may be categorized in the high-risk group for ATL. HTLV-1-specific CTLs evinced vigorous proliferation in *ex vivo* cultures of PBMCs from post-hematopoietic stem cell transplantation (HSCT) patients, but not from pre-HSCT patients (Harashima et al., 2004). Our results in this study show that although HTLV-1-specific CD8+ T-cell response in ATL cells *ex vivo* was not induced by Tax peptide only, CTL response to peptide could be augmented by HTLV-1/HBc particle, leading to specific lysis of cells presenting the appropriate peptide. Harashima et al. (2004) have also reported a similar difficulty in inducing CD8+ cells from ATL patients. Indeed, CD8+ T-cell response can be quite varied among patients, as seen for positive responses even in the absence of peptide, possibly due to reaction to self-antigen, or no response to antigen stimulation in our assay system, suggesting possible immune exhaustion due to relative antigen excess. Induction of an adequate HTLV-1-specific cellular immune response may significantly reduce HTLV-1 proviral load as has been reported in a squirrel monkey model of HTLV-1 infection (Kazanji et al., 2006). Imperatively, therefore, protection against ATL development in chronic HTLV-1 carriers may be afforded by the induction of HTLV-1-specific CTLs. The efficient induction of HTLV-1-specific CTL by HTLV-1/HBc chimera particle could also be adapted to prevent the relapse of ATL in post-HSCT patients.

In this study, we have demonstrated that the HTLV-1/HBc chimeric particle enhanced DC maturation in HLA-A*0201-transgenic mice. These activated DCs, in turn, strongly induced the HTLV-1-specific CD8+ T-cell response without adjuvant. These results suggest that HTLV-1/HBc chimeric particle without adjuvant is capable of inducing strong cellular immune responses via effective dendritic cell maturation, and is potentially useful as an effective therapeutic vaccine model against tumors and infectious diseases by substituting the epitope peptide.

Conflict of interest

No potential conflicts of interest relevant to this article.

Acknowledgements

Grant supports: This work was supported in part by a Grant-in-Aid (to NA and TK) from the Japanese Ministry of Health, Labor, and Welfare, and by the Kagoshima University for Frontier Science Research Center Program (to NA).

We thank Mr. Aikawa, Mr. Shoji and Mrs. Higashi for technical assistance, and Mr. Toji for providing tetramer reagents.

References

Albert, M.L., Sauter, B., Bhardwaj, N., 1998. Dendritic cells acquire antigen from apoptotic cells and induce class I-restricted CTLs. Nature 392, 86–89.

Aubry, J.P., Blaecke, A., Lecoanet-Henchoz, S., Jeannin, P., Herbault, N., Caron, G., Moine, V., Bonnefoy, J.Y., 1999. Annexin V used for measuring apoptosis in the early events of cellular cytotoxicity. Cytometry 37, 197–204.

Banchereau, J., Steinman, R.M., 1998. Dendritic cells and the control of immunity. Nature 392, 245–252.

Bangham, C.R., 2008. HTLV-1 infection: role of CTL efficiency. Blood 112, 2176–2177.

Da Silva, D.M., Fausch, S.C., Verbeek, J.S., Kast, W.M., 2007. Uptake of human papillomavirus virus-like particles by dendritic cells is mediated by Fcgamma receptors and contributes to acquisition of T cell immunity. J. Immunol. 178, 7587–7597.

Grgacic, E.V., Anderson, D.A., 2006. Virus-like particles: passport to immune recognition. Methods 40, 60–65.

Harashima, N., Kurihara, K., Utsunomiya, A., Tanosaki, R., Hanabuchi, S., Masuda, M., Ohashi, T., Fukui, F., Hasegawa, A., Masuda, T., Takaue, Y., Okamura, J., Kannagi, M., 2004. Graft-versus-Tax response in adult T-cell leukemia patients after hematopoietic stem cell transplantation. Cancer Res. 64, 391–399.

Imamura, T., Araki, M., Miyanohara, A., Nakao, J., Yonemura, H., Ohtomo, N., Matsubara, K., 1987. Expression of hepatitis B virus middle and large surface antigen genes in Saccharomyces cerevisiae. J. Virol. 61, 3543–3549.

Jacobson, S., Shida, H., McFarlin, D.E., Fauci, A.S., Koenig, S., 1990. Circulating CD8+ cytotoxic T lymphocytes specific for HTLV-I pX in patients with HTLV-I associated neurological disease. Nature 348, 245–248.

Kawakami, Y., Fujita, T., Kudo, C., Sakurai, T., Udagawa, M., Yaguchi, T., Hasegawa, G., Hayashi, E., Ueda, Y., Iwata, T., Wang, Q., Okada, S., Tsukamoto, N., Matsuzaki, Y., Sumimoto, H., 2008. Dendritic cell based personalized immunotherapy based on cancer antigen research. Front. Biosci. 13, 1952–1958.

Kazanji, M., Heraud, J.M., Merien, F., Pique, C., de The, G., Gessain, A., Jacobson, S., 2006. Chimeric peptide vaccine composed of B- and T-cell epitopes of human T-cell leukemia virus type 1 induces humoral and cellular immune responses and reduces the proviral load in immunized squirrel monkeys (Saimiri sciureus). J. Gen. Virol. 87, 1331–1337.

Komori, H., Nakatsura, T., Senju, S., Yoshitake, Y., Motomura, Y., Ikuta, Y., Fukuma, D., Yokomine, K., Harao, M., Beppu, T., Matsui, M., Torigoe, T., Sato, N., Baba, H., Nishimura, Y., 2006. Identification of HLA-A2- or HLA-A24-restricted CTL epitopes possibly useful for glypican-3-specific immunotherapy of hepatocellular carcinoma. Clin. Cancer Res. 12, 2689–2697.

Kozako, T., Arima, N., Toji, S., Masamoto, I., Akimoto, M., Hamada, H., Che, X.F., Fujiwara, H., Matsushita, K., Tokunaga, M., Haraguchi, K., Uozumi, K., Suzuki, S., Takezaki, T., Sonoda, S., 2006. Reduced frequency, diversity, and function of human T cell leukemia virus type 1-specific CD8+ T cell in adult T cell leukemia patients. J. Immunol. 177, 5718–5726.

Kozako, T., Yoshimitsu, M., Fujiwara, H., Masamoto, I., Horai, S., White, Y., Akimoto, M., Suzuki, S., Matsushita, K., Uozumi, K., Tei, C., Arima, N., 2009. PD-1/PD-L1 expression in human T-cell leukemia virus type 1 carriers and adult T-cell leukemia/lymphoma patients. Leukemia 23, 375–382.

Milich, D.R., McLachlan, A., Thornton, G.B., Hughes, J.L., 1987. Antibody production to the nucleocapsid and envelope of the hepatitis B virus primed by a single synthetic T cell site. Nature 329, 547–549.

Miyanohara, A., Imamura, T., Araki, M., Sugawara, K., Ohtomo, N., Matsubara, K., 1986. Expression of hepatitis B virus core antigen gene in Saccharomyces cerevisiae: synthesis of two polypeptides translated from different initiation codons. J. Virol. 59, 176–180.

Pascolo, S., Bervas, N., Ure, J.M., Smith, A.G., Lemonnier, F.A., Perarnau, B., 1997. HLA-A2.1-restricted education and cytolytic activity of CD8(+) T lymphocytes from beta2 microglobulin (beta2m) HLA-A2.1 monochain transgenic H-2Db beta2m double knockout mice. J. Exp. Med. 185, 2043–2051.

Qian, J., Dong, Y., Pang, Y.Y., Ibrahim, R., Berzofsky, J.A., Schiller, J.T., Khleif, S.N., 2006. Combined prophylactic and therapeutic cancer vaccine: enhancing CTL responses to HPV16 E2 using a chimeric VLP in HLA-A2 mice. Int. J. Cancer 118, 3022–3029.

Senju, S., Hirata, S., Matsuyoshi, H., Masuda, M., Uemura, Y., Araki, K., Yamamura, K., Nishimura, Y., 2003. Generation and genetic modification of dendritic cells derived from mouse embryonic stem cells. Blood 101, 3501–3508.

Shiosaki, K., Takata, K., Nishimura, S., Mizokami, H., Matsubara, K., 1991. Production of hepatitis B virion-like particles in yeast. Gene 106, 143–149.

Storni, T., Lechner, F., Erdmann, I., Bachi, T., Jegerlehner, A., Dumrese, T., Kundig, T.M., Ruedl, C., Bachmann, M.F., 2002. Critical role for activation of antigen-presenting

cells in priming of cytotoxic T cell responses after vaccination with virus-like particles. J. Immunol. 168, 2880–2886.
Uchiyama, T., 1997. Human T cell leukemia virus type I (HTLV-I) and human diseases. Annu. Rev. Immunol. 15, 15–37.
Yasunaga, J., Sakai, T., Nosaka, K., Etoh, K., Tamiya, S., Koga, S., Mita, S., Uchino, M., Mitsuya, H., Matsuoka, M., 2001. Impaired production of naive T lymphocytes in human T-cell leukemia virus type I-infected individuals: its implications in the immunodeficient state. Blood 97, 3177–3183.
Zhang, S., Cubas, R., Li, M., Chen, C., Yao, Q., 2009. Virus-like particle vaccine activates conventional B2 cells and promotes B cell differentiation to IgG2a producing plasma cells. Mol. Immunol. 46, 1988–2001.
Zhang, Y., Song, S., Liu, C., Wang, Y., Xian, X., He, Y., Wang, J., Liu, F., Sun, S., 2007. Generation of chimeric HBc proteins with epitopes in E. coli: formation of virus-like particles and a potent inducer of antigen-specific cytotoxic immune response and anti-tumor effect in vivo. Cell. Immunol. 247, 18–27.

Int J Hematol (2009) 89:188–194
DOI 10.1007/s12185-008-0233-x

CASE REPORT

Uncommon cases of immature-type CD56$^+$ natural killer (NK)-cell neoplasms, characterized by expression of myeloid antigen of blastic NK-cell lymphoma

Satsuki Owatari · Maki Otsuka · Taketsugu Takeshita · Kyoko Mizukami · Sinsuke Suzuki · Kimiharu Uozumi · Yukie Tashiro · Naomichi Arima · Shuichi Hanada

Received: 3 April 2008 / Revised: 30 September 2008 / Accepted: 18 November 2008 / Published online: 25 December 2008

Abstract Immature-type CD56$^+$ natural killer (NK)-cell neoplasms are classified as either myeloid/NK-cell precursor acute leukemia or blastic NK-cell lymphoma. We identified two cases of immature-type CD56$^+$ NK-cell neoplasms that were not categorizable as either of these entities. The first case involved a 74-year-old woman presenting with skin eruptions and pancytopenia due to bone marrow necrosis. Skin biopsy specimen revealed CD4$^+$, CD7$^-$, CD34$^-$, CD43$^+$, CD56$^+$, CD68$^+$, muramidase (lysozyme)$^+$, and myeloperoxidase (MPO)$^-$, and immunophenotyping of peripheral blood showed CD4$^+$, CD7$^-$, CD13$^+$, CD33$^+$, CD34$^-$, CD43$^+$, CD56$^+$, cytoplasmic (cy)CD68$^+$, CD123$^+$, and HLA-DR$^+$. The second case involved a 62-year-old man who had bilateral optic nerve tumor and presented with malignant cells in peripheral blood. Cell surface markers of malignant cells showed CD4$^+$, CD7$^-$, CD13$^+$, CD33$^+$, CD34$^-$, CD43$^+$, CD56$^+$, cyCD68$^+$, and HLA-DR$^+$. The phenotypes of tumor cells in both cases were compatible with blastic NK-cell lymphoma, except for the expression of myeloid antigen. Clinical presentations of these cases showed characteristics of both blastic NK-cell lymphoma and myeloid/NK-cell precursor acute leukemia.

Keywords Blastic NK-cell lymphoma · Myeloid/NK-cell precursor acute leukemia · Myeloid/NK-cell acute leukemia · Plasmacytoid dendritic cells

S. Owatari (✉) · M. Otsuka · T. Takeshita · K. Mizukami · S. Hanada
Department of Internal Medicine, National Hospital Organization Kagoshima Medical Center, 8-1 Shiroyama, Kagoshima 892-0853, Japan
e-mail: owatari@kagomc2.hosp.go.jp

S. Owatari · S. Suzuki · K. Uozumi · N. Arima
Department of Hematology and Immunology, Kagoshima University, 8-35-1 Sakuragaoka, Kagoshima 890-8520, Japan

Y. Tashiro
Department of Pathology, Imakiire General Hospital, 4-16 Shimotatsuo-cho, Kagoshima 892-8502, Japan

1 Introduction

Natural killer (NK) cells are defined as lymphocytes mediating major histocompatibility complex (MHC)-nonrestricted cytotoxicity and show variable expression of CD16, CD56, CD57, T-cell intracellular antigen (TIA)-1, perforin and granzyme B [1]. Several NK/T-cell neoplasms have been reported according to the 2001 World Health Organization (WHO) classifications: blastic NK-cell lymphoma; aggressive NK-cell leukemia; and nasal-type extranodal NK/T-cell lymphoma [2]. In 1994, Scott et al. proposed 20 cases of myeloid/NK-cell acute leukemia from 350 cases of adult de novo acute myeloid leukemia that showed HLA-DR$^-$, CD33$^+$, CD56$^+$, and CD16$^-$ phenotypes [3]. In 1997, Suzuki et al. reported myeloid/NK-cell precursor acute leukemia characterized by the expression of CD7, CD33, CD34, CD56, and HLA-DR proteins, and aggressiveness of the disease [4, 5]. Among these CD56$^+$ NK neoplasms, the immature types are blastic NK-cell lymphoma and myeloid/NK-cell precursor acute leukemia. CD56 is defined as a neural cell adhesion molecule that functions in cell-to-cell adhesion and is reportedly associated with cell homing mechanisms and patterns of malignant cell dissemination [6]. Blastic NK-cell lymphoma is defined phenotypically by positive results for CD4, CD43, CD56, CD68, and CD123 and negative results for conventional myeloid and lymphoid T- and B-cell markers, with general

involvement of the skin in most cases [7–9]. In our cases, classification according to these features was difficult, as immunophenotypical and clinical presentations did not coincide with either myeloid/NK-cell precursor acute leukemia or blastic NK-cell lymphoma. Immunophenotypically, these cases resembled blastic NK-cell lymphoma, but myeloid antigen expression in these cases differed substantially. In terms of clinical presentation, our cases possessed characteristics of both myeloid/NK-cell precursor acute leukemia and blastic NK-cell lymphoma.

2 Materials and methods

2.1 Immunohistochemistry

Immunohistochemical staining of skin biopsy tissue in Case 1 was performed using the avidin–biotin peroxidase complex technique with a Vectastain ABC Elite Kit (Vector Laboratories, Burlingame, CA, USA) and DAB (Dojindo Laboratories, Kumamoto, Japan) or a New Fuchsin Substrate System (Dako, Carpinteria, CA, USA) for visualization of binding. The antibodies used are listed in Table 1. In situ hybridization for Epstein-Barr virus (EBV)-encoded small RNA-1 (EBER-1) was performed using formalin-fixed, paraffin-embedded sections according to the instructions with the DIG Nucleic Acid Detection Kit (Boehringer Mannheim, Marburg, Germany). Digoxigenin-labeled oligonucleotide probes for EBER-1 (labeled using a DIG Oligonucleotide 3'-End Labeling Kit; Japan Bio Services, Saitama, Japan) was used.

2.2 Flow cytometry

Three-color flow cytometry was performed on a FACScan (Becton Dickinson, Mountain View, CA, USA) as described. Flow-cytometric analysis of peripheral blood antigen in both cases was accomplished in accordance with the instructions from the manufacturer. Fluorochrome-conjugated antibodies used for flow cytometry are summarized in Table 1.

2.3 Gene rearrangement studies

Briefly, DNA was isolated from peripheral blood in both cases, subjected to restriction endonuclease digestion with *Bam*HI, *Eco*RV and *Hin*dIII, electrophoresed through agarose, transferred to nylon membranes, then hybridized with a T-cell receptor (TCR) probe.

2.4 Molecular analysis

Southern blot analysis was performed using a previously described technique [10]. Briefly, following extraction from peripheral blood in Case 2, DNA was digested with the *Bam*HI restriction endonuclease, resolved by agarose gel electrophoresis, and transferred to a nylon membrane that then probed with DNA probe specific for EBV terminal repeat sequences (*Xho*I).

3 Patients

3.1 Case 1

In February 2005, a 74-year-old woman suffered skin eruptions and consulted a dermatologist. The skin lesion was not responsive to ordinary treatment, so skin biopsy was performed. Within 1 week after biopsy, before biopsy results were obtained, general condition and level of consciousness gradually deteriorated. Hemorrhage of the oral cavity and petechiae of the extremities were observed. In March 2005, she was referred to our department. On admission, white blood cell (WBC) count was 2.74 $\times$ 10^9/l (neutrophils, 77.0%; lymphocytes, 7.0%; monocytes, 8.0%; basophils, 1.0%; abnormal lymphocytes, 7.0%), hemoglobin level was 14.8 g/dl, platelet count was 14.0 $\times$ 10^9/l, aspartate aminotransferase level was 74 IU/l, alanine aminotransferase level was 52 IU/l, lactate dehydrogenase (LDH) level was 6,895 IU/l (normal, 119–229 IU/l), alkaline phosphatase level was 4,725 IU/l (normal, 115–359 IU/l), C-reactive protein (CRP) level was 43.22 mg/dl, prothrombin time-international normalized ratio (PT-INR) was 1.30, fibrinogen level was 454 mg/dl (normal, 150–400 mg/dl) and fibrinogen degradation product level was 397.71 μg/ml (normal, < 5 μg/ml). Bone marrow examination from iliac bone showed necrotic bone marrow, so diagnosis based on bone marrow samples was not possible. Physical examination revealed no lymphadenopathy or hepatosplenomegaly. Considering the laboratory data and clinical symptoms on admission, severe bacterial infections and disseminated intravascular coagulation (DIC) were diagnosed, and undetermined concomitant hematological malignancy was suspected. Meropenem and nafamostat mesilate were thus initiated for infection and DIC, respectively. Skin biopsy revealed tumor cells with irregular nuclei, and infiltration was observed from the upper dermis to the deep dermis (Fig. 1a). In addition, three possible diagnoses were indicated: blastic NK-cell lymphoma; myeloid/NK-cell precursor acute leukemia; or acute myelomonoblastic leukemia (AMMoL). Immunohistochemical analysis of skin biopsy indicated $CD1^-$, $CD3^-$, $CD4^+$, $CD5^-$, $CD7^-$, $CD8^-$, $CD10^-$, $CD15^+$, $CD30^-$, $CD34^-$, $CD43^+$, $CD56^+$, $CD68^+$, $CD79a^-$, $Ki67^+$, $muramidase^+$, MPO^-, terminal deoxynucleotidil transferase $(TdT)^-$, and $TIA\text{-}1^-$ (Fig. 1b). We could not confirm the diagnosis at this point due to the complex

Table 1 Antibodies used for immunohistochemistry and flow cytometry

Antibodies used for immunohistochemistry			Antibody used for flow cytometry		
Marker	Clone	Source	Marker	Clone	Source
CD1a	MTB1	Novocastra	CD1	NA1/34	Dako
CD3	PS1	Novocastra	CD2	T11	Beckman Coulter
CD4	1F6	Novocastra	CD3	UCHT1	Beckman Coulter
CD5	4C7	Novocastra	CD4	T4	Beckman Coulter
CD7	CD7-272	Novocastra	CD5	T1	Beckman Coulter
CD8	1A5	MBL	CD7	3A1	Beckman Coulter
CD10	56C6	Novocastra	CD8	T8	Beckman Coulter
CD15	MCS-1	Nichirei	CD10	J5	Beckman Coulter
CD30	Ber-H2	Dako	CD11c	BU15	Immunotech
CD34	My10	Becton Dickinson	CD13	WM47	Dako
CD43	DF-T1	Dako	CD15	VIMC6	Invitrogen
CD56	1B6	Novocastra	CD16	3G8	Dako
cyCD68	PG-M1	Dako	CD19	B4	Beckman Coulter
CD79α	JCB117	Dako	CD20	B-Ly1	Dako
Ki67	MM1	Novocastra	CD23	MHM6	Dako
TdT	Polyclonal	Dako	CD25	2A3	Becton Dickinson
TIA-1	2G9	Immunotech	CD30	Ber-H2	Dako
MPO	Polyclonal	Dako	CD33	WM53	BD Phamingenn
			CD34	581.0	Immunotech
			CD36	FA6-152	Immunotech
			CD43	DF-T1	Dako
			CD56	NKH-1	Beckman Coulter
			cyCD68	Ki-M7	Invitrogen
			CD123	9F5	Becton Dickinson
			HLA-DR	Anti-HLADR	Fugisawa Pharma
			TdT	TdT-6	Invitrogen
			κ-chain	TB28-2	Becton Dickinson
			λ-chain	1-155-2	Becton Dickinson
			CLA	HECA-452	BD Phamingenn
			BDCA-2	AC144	Miltenvi Biotec
			TCL-1	H29-1349	BD Biosciences

immunophenotype. Considering the skin biopsy result, we administered CHOP chemotherapy using vincristine (VCR), cyclophosphamide (CPA), doxorubicine (ADM), and prednisolone (PDN). Following these chemotherapies, the skin lesion gradually improved, but was never cured. Skin lesions and hematological data temporarily improved, but rashes gradually worsened again (Fig. 1c). In November 2005, WBC rapidly increased to 30.41 × 10^9/l (abnormal lymphocytes, 62.0%) and LDH level also increased to 1,100 IU/l (Fig. 1d). Flow cytometric analysis of peripheral blood showed $CD2^+$, $CD3^-$, $CD4^+$, $CD5^-$, $CD7^-$, $CD8^-$, $CD10^-$, $CD11c^+$, $CD13^+$, $CD15^+$, $CD16^+$, $CD19^-$, $CD20^-$, $CD23^-$, $CD25^-$, $CD30^-$, $CD33^+$, $CD34^-$, $CD36^+$, $CD43^+$, $CD56^+$, $cyCD68^+$, $CD123^+$, $HLA\text{-}DR^+$, TdT^-, κ-$chain^-$, λ-$chain^-$, and cutaneous lymphocyte antigen $(CLA)^-$ (Table 2). General condition worsened along with the increase in leukocytes, so intensive chemotherapy was initiated according to an acute lymphoblastic leukemia induction regimen with VCR, daunorubicine, CPA and PDN. Despite these therapies, DIC developed and gastrointestinal bleeding occurred, followed by bacterial pneumonia. The patient died in December 2005. Autopsy was not permitted.

3.2 Case 2

In April 2005, a 62-year-old man consulted an ophthalmic hospital complaining of double vision. During examinations, an orbital mass was identified and he was thus referred to the Department of Neurosurgery in our hospital.

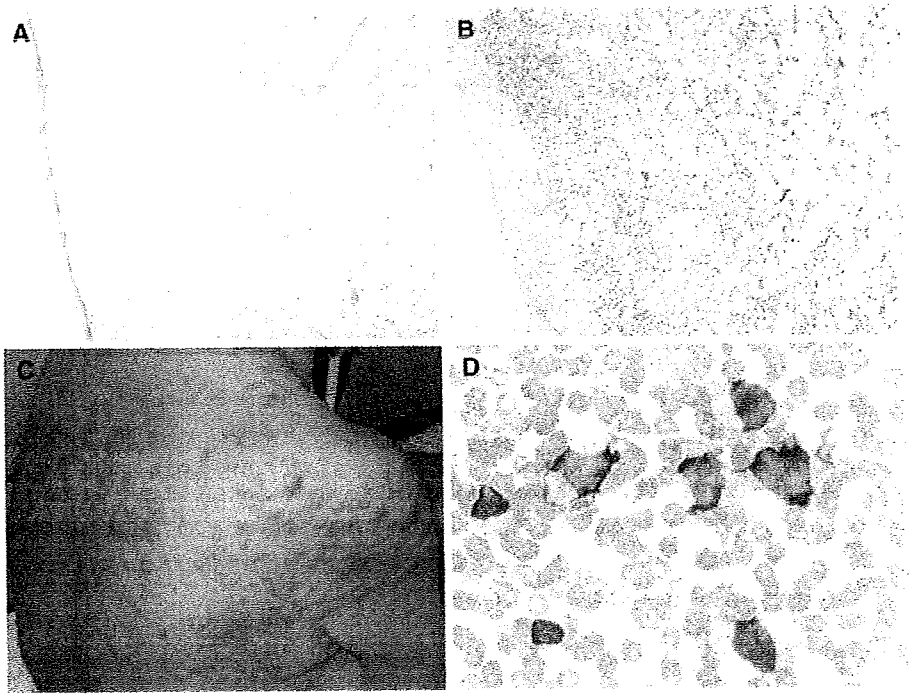

Fig. 1 **a** Skin biopsy specimen in Case 1 showing extensive tumor infiltration from the upper dermis to the deep dermis (hematoxylin–eosin staining, × 100). **b** Skin biopsy specimen in Case 1 showing extensive tumor infiltration expressing CD56 antigen (immunohistochemical staining for CD56, × 100). **c** Skin eruption on the back and shoulder showed disease progression in Case 1. Skin lesions were shown over the whole body including the face and extremities. **d** Peripheral blood smear at disease progression in Case 1 showed large tumor cells with lymphoblastoid morphology and irregularly shaped nuclei without any cytoplasmic granules (May-Grunwald-Giemsa staining, × 1000)

Physical examination revealed cervical lymphadenopathy and magnetic resonance imaging (MRI) identified optic nerve tumors in bilateral orbits (Fig. 2a). Moreover, gallium scintigraphy indicated multiple areas of abnormal uptake in mediastinal, pulmonary hilus, axillary and cervical lymph nodes. Peripheral blood revealed leukemic phase with a WBC count of 28.96 × 10^9/l (neutrophils, 46.0%; lymphocytes, 10.0%; monocytes, 2.0%; abnormal lymphocytes, 42.0%) and an LDH level of 1,132 IU/l (Fig. 2b). Hematological malignancy was suspected and he was referred to our department. Examination of bone marrow from the sternum showed hypoplastic marrow with 37.2% abnormal lymphocytes. Chromosomal karyotyping of bone marrow aspirate was not performed. Cell surface marker analysis of peripheral blood led to suspicion of NK/T cell lymphoma, with results of $CD1^-$, $CD2^-$, $CD3^-$, $CD4^+$, $CD5^-$, $CD7^-$, $CD8^-$, $CD10^-$, $CD11c^+$, $CD13^+$, $CD15^+$, $CD16^-$, $CD19^-$, $CD20^-$, $CD23^-$, $CD25^-$, $CD30^-$, $CD33^+$, $CD34^-$, $CD36^+$, $CD43^+$, $CD56^+$, $cyCD68^+$, $HLA\text{-}DR^+$, TdT^-, κ-$chain^-$, and λ-$chain^-$ (Table 2). These cell surface markers of peripheral blood did not match previously reported NK/T-cell neoplasms. Chemotherapy was initiated with hyper-CVAD [course 1: CPM, VCR, ADM, and dexamethazone (DEX); course 2: methotrexate and cytarabine]. After four course of hyper-CVAD by November 2005, tumors of the optic nerve and all other lesions had disappeared on evaluation with MRI and computed tomography (CT), so complete response was recognized and the patient was discharged. However, WBC count increased again to 37.24 × 10^9/l in January 2006 and LDH also increased to 1,420 IU/l. MRI of the head indicated a large mass lesion in the left temporal lobe and CT indicated systemic multiple lymphadenopathy. As relapse was confirmed, administration of etoposide and DEX was started, but these treatments were ineffective and level of consciousness gradually decreased thereafter due to the brain tumor. The patient died in May 2006. Autopsy was not permitted.

4 Results and discussion

The classification of NK/T-cell neoplasm has been under debate. Immature-type CD56-positive NK-cell neoplasms are blastic NK-cell lymphomas as defined by WHO classifications and myeloid/NK-cell precursor acute leukemia was established by Suzuki et al. [2, 4]. These immature-type NK-cell neoplasms are not associated with EBV infection, and thus differ from other mature-type NK-cell neoplasms, which are highly associated with EBV infection. Exact determination of NK-cell lineage neoplasms by studying TCR expression and/or gene rearrangement is necessary, as CD56 is a marker of both NK cells and a subset of cytotoxic T cells. To exclude the T-cell linage, demonstration of the absence of monoclonal rearrangement of the TCR gene is needed. Both of the present cases showed a lack of TCR rearrangement on Southern blotting, and then were further confirmed by the absence of EBV

Table 2 Immunophenotyping of cell surface marker of the peripheral tumor cells in Case 1 and Case 2

Marker	Case 1	Case 2
CD1	−	−
CD2	+	−
CD3	−	−
CD4	+	+
CD5	−	−
CD7	−	−
CD8	−	−
CD10	−	−
CD11c	+	+
CD13	+	+
CD15	+	+
CD16	+	−
CD19	−	−
CD20	−	−
CD23	−	−
CD25	−	−
CD30	−	−
CD33	+	+
CD34	−	−
CD36	+	+
CD43	+	+
CD56	+	+
cyCD68	+	+
CD123	+	ND
HLA-DR	+	+
TdT	−	−
κ-Chain	−	−
λ-Chain	−	−
CLA	−	ND
BDCA-2	+	−
TCL-1	−	−

HLA-DR human leukocyte antigen, *TdT* terminal deoxynucleotidil transferase, *CLA* cutaneous lymphocyte antigen, *BDCA-2* blood dendritic cells antibodies 2, *TCL-1* T-cell leukemia/lymphoma protein 1, *ND* not done

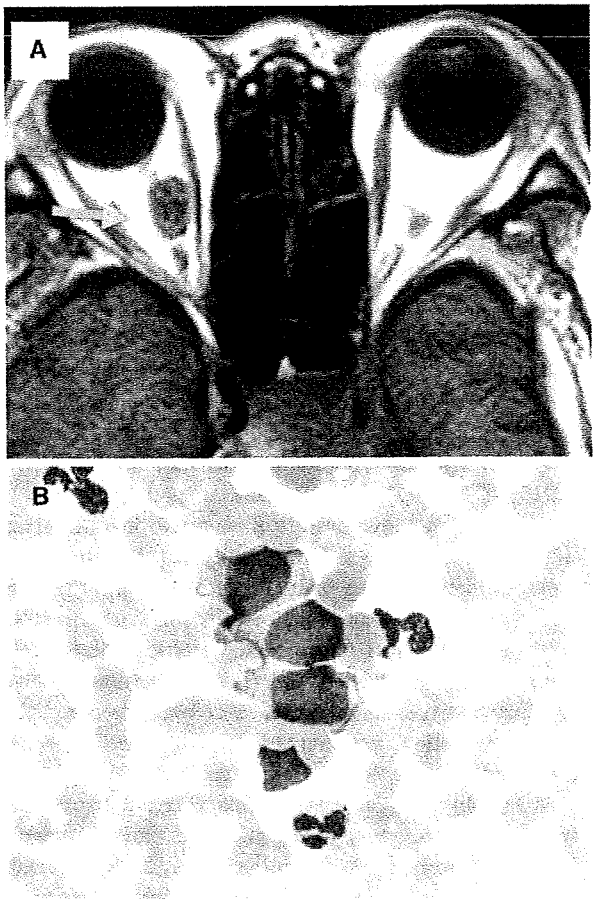

Fig. 2 **a** Magnetic resonance imaging showing optic nerve tumor in the orbit in Case 2. *Yellow arrows* indicate bilateral tumor position. **b** Peripheral blood smear on admission in Case 2 shows large, pleomorphic, lymphoid-like cells with pale cytoplasm and fine cytoplasmic granules (May-Grunwald-Giemsa staining, × 1000)

infection in skin tissue in Case 1 and peripheral blood malignant cells in Case 2. Both cases were therefore diagnosed with immature-type CD56-positive NK-cell neoplasms, but classification was difficult due to the complex immunophenotypes of tumor cells. We have reported herein two unusual CD56-positive NK-cell neoplasms. Possible diagnoses in these cases were blastic NK-cell lymphoma, myeloid/NK-cell precursor leukemia, myeloid/NK-cell acute leukemia, $CD4^+/CD56^+$ hematodermic neoplasm, AMMoL, T-lymphoblastic lymphoma (T-LBL), nasal NK-cell lymphoma and aggressive NK-cell leukemia/lymphoma. Nasal NK-cell lymphoma shows a predilection for nasal or oral cavities, and is almost always associated with EBV [6]. Aggressive NK-cell leukemia/lymphoma initially manifests with lymphadenopathy, hepatosplenomegaly, bone marrow and peripheral blood involvement, and is highly associated with EBV infection [6]. Nasal NK-cell lymphoma and aggressive NK-cell leukemia/lymphoma can thus be excluded from our two cases based on negative findings for EBV infection and clinical presentation. About 80% of T-LBL cases begin with a ventral mediastinal tumor, generally originating from the thymus, TdT is almost always expressed and the majority of cases occur in children or young adults [11]. Conversely, median age at diagnosis of blastic NK-cell lymphoma is reportedly 65.3 years [7]. T-LBL can thus be excluded for the present cases based on differences in TdT expression and age of disease occurrence.

Skin biopsy specimen in Case 1 revealed $CD4^+$, $CD7^-$, $CD15^+$, $CD43^+$, $CD56^+$, $CD68^+$, muramidase$^+$, and

MPO$^-$. When disease progression was noted in Case 1, immunophenotyping of peripheral blood was performed, indicating CD4$^+$, CD7$^-$, CD13$^+$, CD33$^+$, CD34$^-$, CD43$^+$, CD56$^+$, cyCD68$^+$, CD123$^+$ and HLA-DR$^+$, compatible with blastic NK-cell lymphoma, except for myeloid antigen expression. In Case 2, immunophenotyping of peripheral blood on admission was CD4$^+$, CD7$^-$, CD13$^+$, CD33$^+$, CD34$^-$, CD43$^+$, CD56$^+$, cyCD68$^+$, and HLA-DR$^+$, similar to the results for Case 1 without undetermined CD123. In contrast, CD7 expression is indispensable for myeloid/NK-cell precursor acute leukemia, as CD7 is specified in the disease definition, so this diagnosis was able to be ruled out. AMMoL was another differential diagnosis, given positive results for CD15, CD68 and muramidase in skin tissue in Case 1 and CD13, CD15, CD33, and CD68 in peripheral blood in both cases. Moreover, myelomonocytic disorders sometimes express CD4 and CD56 antigens [7]. In both cases, myeloid markers were strongly positive and also showed positive NK-cell markers. However, MPO stain of tumor cells in skin tissue in Case 1 and peripheral blood in Case 2 yielded negative results, whereas such staining is always positive in myeloid leukemia. Moreover, the morphology of tumor cells in peripheral blood in Case 1 was lymphoblastoid morphology with irregularly shaped nuclei without any cytoplasmic granules (Fig. 1d). In Case 2, tumor cells were morphologically identified as lymphoid-like cells with pale cytoplasm and fine cytoplasmic granules, and clinically presented systemic lymphadenopathy including optical nerve tumor (Fig. 2b). According to MPO stain, cell morphology and clinical symptoms, we could rule out AMMoL. Scott et al. presented myeloid antigen-positive NK-cell neoplasm in which myeloid/NK-cell acute leukemia is manifested by the presence of HLA-DR$^-$, CD33$^+$, CD56$^+$, and CD16$^-$ phenotypes, characterizing mature myeloid morphology by the presence of CD33 [3]. HLA-DR was positive in our cases, so that entity did not match on this point. Regarding clinical symptoms, myeloid/NK-cell precursor acute leukemia more frequently involves the bone marrow and lymph nodes, while blastic NK-cell lymphoma affects mainly the skin [12–15]. Case 1 manifested extensive bone marrow infiltration of tumor cells that led to bone marrow necrosis and also showed severe systemic skin lesions. We thus recognize that Case 1 possessed characteristics of both myeloid/NK-cell precursor acute leukemia and blastic NK-cell lymphoma. Blastic NK-cell lymphoma may occasionally be positive for CD33, CD36, and CD38 antigens, but positive findings for both CD13 and CD33 as in thus case has not previously been reported [16]. In Case 2, optic nerve and central nervous system invasion manifested during the clinical course, while CD56$^+$ hematolymphoid malignant neoplasms in general display preferential involvement of extranodal sites, such as skin, the central nervous system and the nasopharynx [17]. Recently, a normal counterpart of blastic NK-cell lymphoma has been reported in type 2 dendritic cells, particularly in CD123 (IL-3α receptor)-positive plasmacytoid dendritic cells (pDCs). In addition, pDCs that express CD4, CD123, HLA-DR, CD43, CD68, and CLA have been mentioned [7, 18]. According to previous reports, CD123 is expressed in few normal cells, but is generally strongly expressed in blastic NK-cell lymphoma [7]. The normal counterparts in Case 1 thus seem likely to be pDCs, as CD123 expression was detected. Moreover, CD4, CD43, CD68 and HLA-DR expression in our case coincided with the immunophenotype of pDCs. More recently, blood dendritic cell antibodies (BDCA-2) and lymphoid proto-oncogen T-cell lymphoma 1 (TCL1) have been identified as a new class of highly specific markers for dendritic cells and appear likely to prove very helpful for the identification of distinct dendritic cell subsets [19, 20]. We examined the expression of these antigens in peripheral blood tumor cells. BDCA-2 was positive only in Case 1, with TCL-1 negative in both cases. These results suggest that the counterpart cells in Case 1 were pDCs, although no counterpart could be identified by flow cytometric analysis in Case 2.

Recently, instead of blastic NK-cell lymphoma, CD4$^+$/CD56$^+$ hematodermic neoplasm (HN) has been suggested as a more appropriate term for derivation from a pDC precursor [21]. CD4$^+$/CD56$^+$HN shows a distinct clinical presentation of primary skin lesion and is generally characterized as immunophenotypically positive for CD4, CD56, and CD43 with variable positivity for TdT and CD68, and negative results for T- and B-cell markers, myeloperoxidase, CD34, and CD10. Both our cases differed from this criterion with negativity for TdT in both cases, and absence of a primary skin lesion in Case 2. The two cases described may well represent different entities, as each case presented some differences in immunophenotypings and clinical presentation. However, neither case coincided with previously reported categories, so we categorized both cases as atypical blastic NK-cell lymphoma.

Several groups have reported uncommon types of immature-type NK-cell neoplasms with immunophenotypical characteristics overlapping between myeloid/NK-cell precursor acute leukemia and blastic NK-cell lymphoma [13, 14]. Controversy remains regarding immature NK/T-cell neoplasms. To date, we have been unable to adequately classify these rare diseases. We and several groups have encountered difficulties in diagnosing these unusual immunophenotypical features of NK/T-cell neoplasms. To elucidate the definitive characteristics of immature NK/T-cell neoplasms, further rare cases must be accumulated and analyzed.

References

1. Oshimi K. NK cell lymphoma. Int J Hematol. 2002;76:118–21.
2. Jaffe ES, Harris NL, Stein H, Vardiman JW. WHO classification of tumors. Pathology and genetics of tumors of haematopoietic and lymphoid tissues. Lyon: IARC Press; 2001.
3. Scott AA, Head DR, Kopecky KJ, Appelbaum FR, Theil KS, Grever MR, et al. HLA-DR$^-$, CD33$^+$, CD56$^+$, CD16$^-$ myeloid/natural killer cell acute leukemia: a previously unrecognized form of acute leukemia potentially misdiagnosed as French-American-British acute myeloid leukemia-M3. Blood. 1994;84:244–55.
4. Suzuki R, Yamamoto K, Seto M, Kagami Y, Ogura M, Yatabe Y, et al. CD7 + and CD56 + myeloid/natural killer cell precursor acute leukemia: a distinct hematolymphoid disease entity. Blood. 1997;90:2417–28.
5. Suzuki R, Nakamura S. Malignancies of natural killer (NK) cell precursor: myeloid/NK cell precursor acute leukemia and blastic NK cell lymphoma/leukemia. Leuk Res. 1999;23:615–24. doi:10.1016/S0145-2126(98)00194-5.
6. Cheung MMC, Chan JKC, Wong K. Natural killer cell neoplasms: a distinctive group of highly aggressive lymphomas/leukemias. Semin Hematol. 2003;40:221–32. doi:10.1016/S0037-1963(03)00136-7.
7. Petrella T, Bagot M, Willemze R, Beylot-Barry M, Vergier B, Delaunay M, et al. Blastic NK-cell lymphomas (agranular CD4 + CD56 + hematodermic neoplasms). Am J Clin Pathol. 2005;123:662–75. doi:10.1309/GJWNPD8HU5MAJ837.
8. Khoury JD, Medeiros LJ, Manning JT, Sulak LE, Bueso-Ramos C, Jones D. CD56$^+$ TdT$^+$ blastic natural killer cell tumor of the skin: a primitive systemic malignancy related to myelomonocytic leukemia. Cancer. 2002;94:2401–8. doi:10.1002/cncr.10489.
9. Ginarte M, Abalde MT, Peteiro C, Fraga M, Alonso N, Toribio J. Blastoid NK cell leukemia/lymphoma with cutaneous involvement. Dermatology. 2000;201:268–71. doi:10.1159/000018475.
10. Raab-Traub N, Flynn K. The structure of the termini of the Epstein-Barr virus as a marker of clonal cellular proliferation. Cell. 1986;47:883–9. doi:10.1016/0092-8674(86)90803-2.
11. Koita H, Suzumiya J, Ohshima K, Takeshita M, Kimura N, Kikuchi M, et al. Lymphoblastic lymphoma expressing natural killer cell phenotype with involvement of the mediastinum and nasal cavity. Am J Surg Pathol. 1997;21:242–8. doi:10.1097/00000478-199702000-00016.
12. Alvarez-Larrán A, Villamor N, Hernandez-Boluda JC, Ferrer A, Camos M, Campo E, et al. Blastic natural killer cell leukemia/lymphoma presenting as overt leukemia. Clin Lymphoma. 2001;2:178–82. doi:10.3816/CLM.2001.n.024.
13. Argyrakos T, Rontogianni D, Karmiris T, Kapsimali V, Grigoriou E, Tsantekidou M, et al. Blastic natural killer (NK)-cell lymphoma: report of an unusual CD4 negative case and review of the CD4 negative neoplasms with blastic features in the literature. Leuk Lymphoma. 2004;45:2127–33. doi:10.1080/10428190410001723232.
14. Sun T, Pashaei S, Jaffrey I, Ryder J. A hybrid form of myeloid/NK-cell acute leukemia and myeloid/NK-cell precursor acute leukemia. Hum Pathol. 2003;34:504–8. doi:10.1016/S0046-8177(03)00087-X.
15. Chen VM, McIlroy K, Loui JP, Fay K, Ward C. Extramedullary presentation of acute leukemia: a case of myeloid/natural killer cell precursor leukemia. Pathology. 2003;35:325–9. doi:10.1080/0031302031000150489.
16. Yang X, Wasserman PG, Bhargava A, Iqbal U, Ragnauth S, Fuchs A. Challenge in diagnosis of CD56$^+$ lymphoproliferative disorders. Arch Pathol Lab Med. 2004;128:100–3.
17. Wong KF, Chan JK, Ng CS, Lee KC, Tsang WY, Cheung MM. CD56(NKH1)-positive hematolymphoid malignancies: an aggressive neoplasm featuring frequent cutaneous/mucosal involvement, cytoplasmic azurophilic granules, and angiocentricity. Hum Pathol. 1992;23:798–804. doi:10.1016/0046-8177(92)90350-C.
18. Chaperot L, Bendriss N, Manches O, Gressin R, Maynadie M, Trimoreau F, et al. Identification of a leukemic counterpart of the plasmacytoid dendritic cells. Blood. 2001;97:3210–7. doi:10.1182/blood.V97.10.3210.
19. Jaye DL, Geigerman CM, Herling M, Eastburn K, Waller EK, Jones D. Expression of the plasmacytoid dendritic cell marker BDCA-2 supports a spectrum of maturation among CD4 + CD56 + hematodermic neoplasms. Mod Pathol. 2006;19:1555–62. doi:10.1038/modpathol.3800679.
20. Herling M, Teitell MA, Shen RR, Medeiros LJ, Jones D. TCL1 expression in plasmacytoid dendritic cells (DC2 s) and the related CD4$^+$CD56$^+$blastic tumor of skin. Blood. 2003;101:5007–9. doi:10.1182/blood-2002-10-3297.
21. Niakosari F, Sur M. Agranular CD4 +/CD56 + hematodermic neoplasm. A distinct entity described in the recent world health organization-European organization for research and treatment of cancer classification for cutaneous lymphomas. Arch Pathol Lab Med. 2007;131:149–51.

Leukemia (2009) 23, 375–382

www.nature.com/leu

ORIGINAL ARTICLE

PD-1/PD-L1 expression in human T-cell leukemia virus type 1 carriers and adult T-cell leukemia/lymphoma patients

T Kozako[1,2,6], M Yoshimitsu[3,6], H Fujiwara[3,5], I Masamoto[1], S Horai[1], Y White[1], M Akimoto[3], S Suzuki[1], K Matsushita[3], K Uozumi[1], C Tei[4] and N Arima[1]

[1]*Division of Hematology and Immunology, Center for Chronic Viral Diseases, Graduate School of Medical and Dental Sciences, Kagoshima University, Kagoshima, Japan;* [2]*Department of Biochemistry, Faculty of Pharmaceutical Sciences, Fukuoka University, Fukuoka, Japan;* [3]*Department of Hematology and Immunology, Kagoshima University Hospital, Kagoshima, Japan and* [4]*Department of Cardiovascular, Respiratory and Metabolic Medicine, Graduate School of Medicine, Kagoshima University, Kagoshima, Japan*

Adult T-cell leukemia/lymphoma (ATLL) develops after infection with human T-cell leukemia virus-1 (HTLV-1) after a long latency period. The negative regulatory programmed death-1/programmed death-1 ligand 1 (PD-1/PD-L1) pathway has been implicated in the induction of cytotoxic T-lymphocyte (CTL) exhaustion during chronic viral infection along with tumor escape from host immunity. To determine whether the PD-1/PD-L1 pathway could be involved in the establishment of persistent HTLV-1 infections and immune evasion of ATLL cells in patients, we examined PD-1/PD-L1 expression on cells from 27 asymptomatic HTLV-1 carriers (ACs) and 27 ATLL patients in comparison with cells from 18 healthy donors. PD-1 expression on HTLV-1-specific CTLs from ACs and ATLL patients was dramatically elevated. In addition, PD-1 expression was significantly higher on CD8+ T cells along with cytomegalovirus (CMV)- and Epstein–Barr virus (EBV)-specific CTLs in ATLL patients compared with ACs and control individuals. Primary ATLL cells in 21.7% of ATLL patients expressed PD-L1, whereas elevated expression was not observed in cells from ACs. Finally, in functional studies, we observed that an anti-PD-L1 antagonistic antibody upregulated HTLV-1-specific CD8+ T-cell response. These observations suggest that the PD-1/PD-L1 pathway plays a role in fostering persistent HTLV-1 infections, which may further ATLL development and facilitate immune evasion by ATLL cells.

Leukemia (2009) **23,** 375–382; doi:10.1038/leu.2008.272; published online 2 October 2008

Keywords: human T-cell leukemia virus-1; adult T-cell leukemia/lymphoma; cytotoxic T lymphocytes; programmed death-1; programmed death-ligand 1

Introduction

Adult T-cell leukemia/lymphoma (ATLL) is a highly aggressive peripheral T-cell neoplasm that develops only after long-term chronic infections with human T-cell leukemia virus-1 (HTLV-1).[1–4] Despite recent progress in both chemotherapy and supportive care for hematological malignancies, the prognosis of ATLL is still poor; overall survival at 3 years is only 24%.[5–8]

Correspondence: Dr N Arima, Division of Hematology and Immunology, Center for Chronic Viral Diseases, Graduate School of Medical and Dental Sciences, Kagoshima University, 8-35-1 Sakuragaoka, Kagoshima 890-8544, Japan.
E-mail: nao@m2.kufm.kagoshima-u.ac.jp
This study was carried out at Kagoshima University.
[5]Current address: Ehime University Graduate School of Medicine, Department of Bioregulatory Medicine, Ehime, Japan.
[6]These authors contributed equally to this study.
Received 12 February 2008; revised 23 June 2008; accepted 25 August 2008; published online 2 October 2008

Human T-cell leukemia virus-1 is a human retrovirus that has infected approximately 10–20 million people worldwide, particularly in southern Japan, the Caribbean Basin, South America, Melanesia and Equatorial Africa.[9] Despite this high frequency of human infection, only 2–5% of HTLV-1-infected individuals develop ATLL.[7,10] Multiple factors (for example, virus, host cell and immune factors) have been implicated in the development of ATLL, although the underlying mechanisms of leukemogenesis have not been fully elucidated.[5,8,10] Recently, lines of evidence suggest that HTLV-1-specific cytotoxic T lymphocytes (CTLs) play an important role in suppressing the proliferation of HTLV-1-infected or transformed T cells, and thus may prevent the development of ATLL.[11,12] We have also reported on the reduced frequency and function of HTLV-1 Tax-specific CD8+ T cells in ATLL patients.[13] Taken together, it is thus of great interest to further explore the role of the host T-cell immune system in understanding the persistence of HTLV-1 infections and ATLL leukemogenesis.

The T-cell receptor costimulatory pathways assist in regulating T-cell activation and tolerance.[14–16] The B7-CD28 superfamily membership has been expanded to include costimulatory and inhibitory T-cell receptors, including CD28 and programmed death-1 (PD-1).[15,17] Indeed, studies in PD-1-deficient mice have indicated that PD-1 serves as a negative regulator of immune responses.[18] PD-1 signaling is involved in autoimmunity, allergy, sites of immune privilege and antitumor immunity.[14,16] The interaction of PD-1 with the ligand, programmed death-1 ligand 1 (PD-L1), has been reported to negatively regulate the cytokine production and proliferation of T cells.[14,19,20] Interestingly, PD-L1 expression is also associated with poor prognosis in many cancers, including those of the larynx, lung, stomach, colon, breast, cervix, ovary, renal cell, bladder and liver, as well as in glioma and melanoma.[14] Further, it has been suggested that such tumors may actually evade the host immune system by attenuation of tumor-specific T-cell responses through the PD-1/PD-L1 pathway.[21–23] In addition, PD-1 has recently been shown to be involved in chronic viral infections. For example, Barber *et al.*[24] reported that PD-1 is upregulated in T cells that become exhausted during the chronic phase of viral infection in lymphocytic choriomeningitis virus infected mice. Moreover, blocking the interaction between PD-1 and PD-L1 reactivates the CTL function in those mice.[24] Studies have also suggested that the PD-1/PD-L1 pathway in virus-specific CD8+ T cells may be operating in chronic HIV infection.[25–27] However, there is no report on PD-1 expression in tumor-associated antigen-specific CTLs in humans. Therefore, it is important to explore the association between the PD-1/

PD-L1 pathway and HTLV-1 infection, in terms of both maintenance of the chronic infection and possible effects on the host immune system in this virus-induced malignancy in humans.

In this study, we examined the expression and interaction of PD-1/PD-L1 in asymptomatic HTLV-1 carriers (ACs), ATLL patients and non-HTLV-1-infected individuals to investigate the role of this negative regulatory axis in chronic HTLV-1 infection and associated leukemia.

Materials and methods

Patients

The patients in this study included 27 ACs (24–81 years of age, mean = 59.3), 27 ATLL patients (31–83 years of age, mean = 62.2; two with chronic type, three with lymphoma type and 22 with acute type) and 18 non-HTLV-1-infected healthy donors (HDs; 23–57 years of age, mean = 34.9), all of whom were recruited from the Kagoshima University Hospital. Patients were examined by a standard serological testing for the presence of HTLV-1 and by hematological/Southern blotting analysis for the diagnosis of ATLL. Those patients seropositive for HTLV-1 without clinical symptoms of HTLV-1-related diseases[28] were designated as ACs. Classification of ATLL was made according to Shimoyama's criteria.[29] All patients were inhabitants of Kagoshima prefecture, southern Kyushu and Japan, where ATLL is endemic. All patients gave their written informed consent to participate in this study and to allow review of their medical records, and they also provided a sample of peripheral blood for human leukocyte antigen (HLA) typing and for the HLA tetramer assay. The study protocol was reviewed and approved by the Medical Ethical Committee of Kagoshima University.

Phenotypic analysis

Cells from patients positive for HLA-A*24 were screened by serological staining with monoclonal antibodies (mAbs) for HLA-A*24 subtypes (clone: 17A10; Medical and Biological Laboratories, Nagoya, Japan), followed by secondary staining with goat anti-mouse IgG-fluorescein isothiocyanate (FITC) (Immunotech, Miami, FL, USA) according to the manufacturer's instructions, and subjected to flow cytometry analyses on FACScan (Becton Dickinson, Mountain View, CA, USA). Phenotypic analysis using HLA tetramers was performed as described earlier.[13] Briefly, aliquots of 1×10^6 freshly isolated peripheral blood mononuclear cells (PBMCs) were incubated with the HLA tetramers, FITC-conjugated murine anti-PD-1 mAbs (clone: MIH4; eBioscience, San Diego, CA, USA) and peridinin chlorophyll-a protein-conjugated murine anti-CD8 mAbs (Becton Dickinson, San Jose, CA, USA). Lymphocytes, CD8+ lymphocytes and tetramer-positive CD8+ lymphocytes were analyzed using the FACScan instrument (Becton Dickinson)[30] and FlowJo software (Tree Star, San Carlos, CA, USA).[31] HTLV-1 Tax/HLA tetramers; Tax 301–309 (SFHFLHLLF) with HLA-A*2402 were used in this study (Beckman Coulter Co., Fullerton, CA, USA). Phycoerythrin (PE)-labeled HLA tetramers were produced as described earlier.[32,33] Staining was also performed with an HIV (RYLRDQQLL)/HLA-A*2402 tetramer (Medical and Biological Laboratories) as a negative control, a cytomegalovirus (CMV) (QYDPVAALF)/HLA-A*2402 tetramer and an Epstein–Barr virus (EBV) BRLF1(TYPVLEEMF)/HLA-A*2402 tetramer (Beckman Coulter).[13] We estimated the surface PD-1 expression by subtracting the percentage of isotype control-positive cells from the percentage of anti-PD-1-positive cells. Aliquots of 1×10^6 PBMCs were stained with an FITC-conjugated murine anti-CD25 mAb (Beckman Coulter), a PE-conjugated murine anti-CD4 mAb (Beckman Coulter), a Cy7-conjugated murine anti-PD-L1 mAbs (clone: MIH1; eBioscience) or an isotype control mouse IgG1 antibody (eBioscience). We estimated the surface PD-L1 expression by subtracting the percentage of isotype control-positive cells from the percentage of anti-PD-1-positive cells.

Intracellular Tax, IFN-γ and TNF-α staining assay

Peripheral blood mononuclear cells (1×10^6) for HTLV-1 Tax expression analysis were cultured for 12 h in complete medium (CM; RPMI-1640 supplemented with the following reagents: 100 U/ml penicillin, 0.1 mg/ml streptomycin, 0.05 mM 2-mercaptoethanol, 50 U/ml of recombinant human interleukin-2 and 10% heat-inactivated FCS). PBMCs were labeled with Cy7-conjugated murine anti-PD-L1 mAbs, anti-CD4-PE and anti-CD25-allophycocyanin antibody (Becton Dickinson) for cell-surface antigen analyses.[34] PBMCs (1×10^6) for interferon-γ (IFN-γ) and tumor necrosis factor-α (TNF-α) analyses were cultured for 16 h with or without 0.02 μM HTLV-1 Tax peptide (Sigma Aldrich, Tokyo, Japan) in combination with brefeldin A (Becton Dickinson) in CM. Blocking antibody specific to PD-L1 (clone: MIH1; eBioscience) was added to cell cultures at a concentration of 10 μg/ml.[21,35,36] Cells were collected and labeled with HTLV-1/HLA-tetramer-PE and anti-CD8-allophycocyanin antibodies (Becton Dickinson).[34] These cells were further treated with permeabilizing solution (Becton Dickinson). After washing, the cells were incubated with anti-Tax-FITC (clone: Lt4; kindly provided by Tanaka Y, Ryukyu University), IFN-γ-FITC or TNF-α-FITC antibody (Becton Dickinson). As a negative control, staining was also performed with isotype control IgG1-FITC (Becton Dickinson) for Tax and FastImmune Control γ2aFITC/γ1PE for IFN-γ and TNF-α (Becton Dickinson). Lymphocyte analyses were performed using FACSCalibur and analyzed with FlowJo software.[13]

CD107a mobilization assay

Assessment of cytolytic ability was performed using flow cytometric quantification of the surface mobilization of CD107a—an integral membrane protein in cytolytic granules—as a marker of degranulation after stimulation, as described earlier.[13,37] Briefly, PBMCs (1×10^6) were cultured for 6 h with or without 0.02 μM HTLV-1 Tax peptide (Sigma Aldrich) in combination with anti-CD107a mAbs-FITC (clone: H4A3; Southern Biotech, Birmingham, AL, USA) and the secretion inhibitor monensin (Becton Dickinson) in CM. Blocking antibody specific to PD-L1 (clone: MIH1; eBioscience) was added to cell cultures at a concentration of 10 μg/ml. The cells were further stained with HLA-tetramer-PE and anti-CD8 mAb-PE/Cy5 (Beckman Coulter) as described earlier.[13] Aliquots of 1×10^4 CD8+ T lymphocytes were examined using FACSCalibur and analyzed with FlowJo software.

Statistical analysis

Mann–Whitney- and Wilcoxon-matched pair tests were performed using a StatView software version 5.0 (SAS Institute Inc., Cary, NC, USA). *P*-values of less than 0.05 were considered significant.

Results

PD-1 expression in ACs and ATLL patients

Freshly isolated or cryopreserved PBMCs from 27 ACs and 25 ATLL patients were stained for PD-1 in combination with CD8 and HTLV-1 Tax, CMV or EBV tetramers, allowing for the direct visualization of PD-1 expression on tetramer-positive CD8+ lymphocytes. In this study, the cell-surface phenotype of ATLL cells determined by flow cytometric analyses showed the $CD4^+/CD25^+/CD8^-$ (data not shown). We were able to exclude the contribution of PD-1 expression from ATLL cells by analyzing PD-1 expression on CD8+ cells. PD-1 expression was readily apparent on lymphocytes and tetramer-positive CD8+ T cells (Figure 1). Percentages of total and CD8+ lymphocytes from ACs and ATLL patients expressing PD-1 were significantly higher than those from HDs (Figure 1b, $P<0.01$ and 0.001, respectively). Importantly, percentages of total and CD8+ lymphocytes in ATLL patients who expressed PD-1 were significantly even higher than those from ACs ($P<0.01$). Overall, there was no correlation between age and the rates of PD-1 expression, although ATLL patients with high PD-1 expression were significantly younger than those with low PD-1 expression (58.1 years of age versus 67.3 years of age, $P<0.05$, data not shown).

We next assessed PD-1 expression on viral antigen-specific CD8+ lymphocytes (Figure 1c). The rates of PD-1 expression on CMV- and EBV-tetramer-positive CD8+ lymphocytes from ATLL patients were significantly higher than those in HDs (Figure 1c, $P<0.01$ and 0.005, respectively) and ACs ($P<0.01$ and 0.05, respectively). In contrast, we found that 72.7 ± 27.1% of HTLV-1-tetramer-positive CD8+ lymphocytes from ACs expressed PD-1 and that a similar number of HTLV-1-tetramer-positive lymphocytes from ATLL patients expressed PD-1 ($P=0.32$). Furthermore, PD-1 was expressed on significantly higher percentages of HTLV-1-specific cells as compared with CMV- and EBV-specific CD8+ T cells in ACs ($P<0.01$ and 0.05, respectively), but not in ATLL patients. These observations regarding PD-1 cell-surface expression were unique as we did not observe simultaneous increased cell-surface expression of the inhibitory receptor CTL antigen-4 (data not shown).

PD-L1 expression in ACs and ATLL patients

To explore whether ATLL cells and HTLV-1-infected cells could possibly evade the host immune system by expression of the

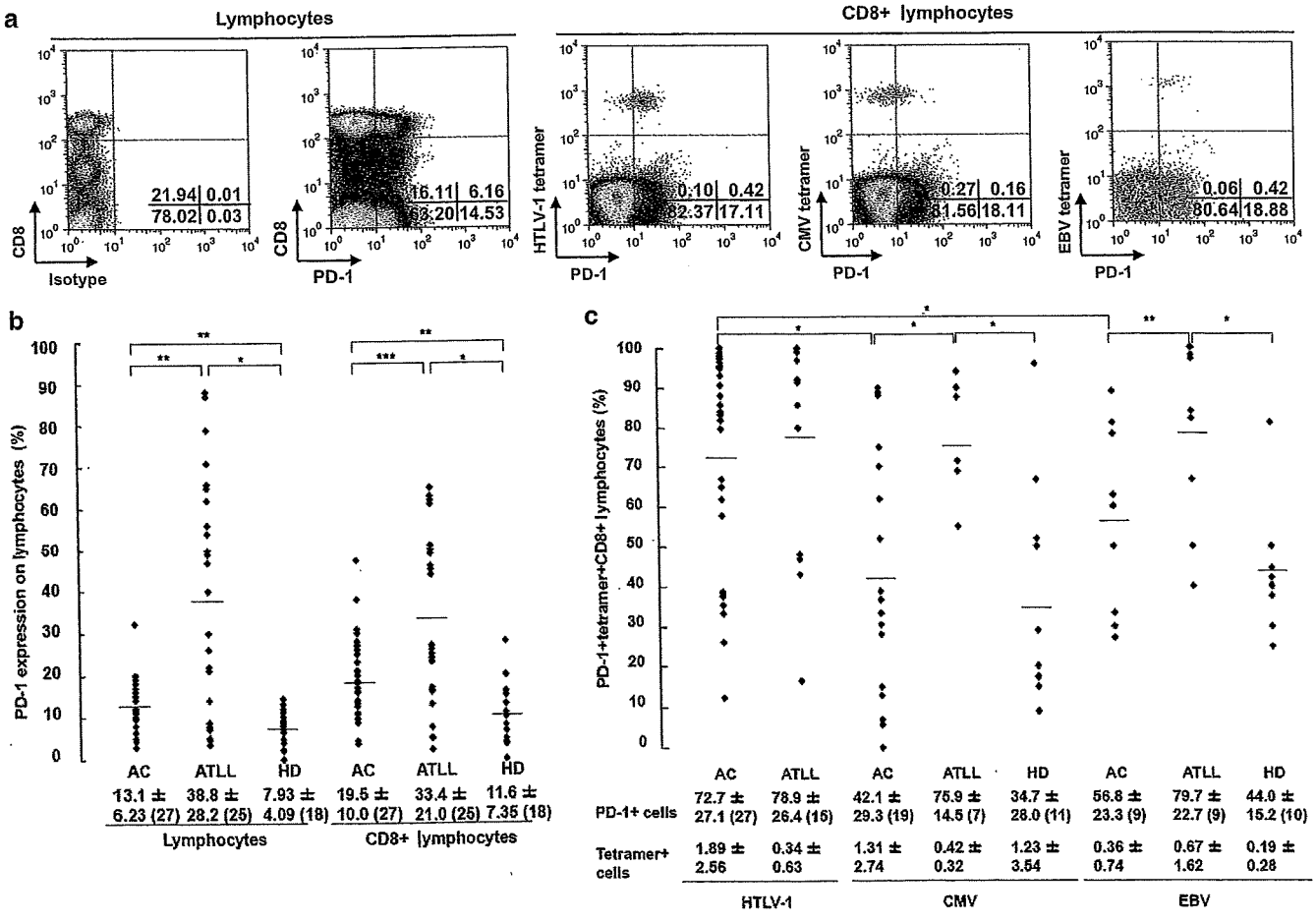

Figure 1 PD-1 expression on virus-specific CD8+ T lymphocytes in asymptomatic HTLV-1 carriers (ACs) and adult T-cell leukemia/lymphoma (ATLL) patients. (**a**) Representative flow cytometric plots of programmed death-1 (PD-1) expression on total lymphocytes and virus-specific CD8+ T lymphocytes in AC. Numbers indicate the percentages of lymphocytes or CD8+ T lymphocytes. (**b**) Percentage of PD-1 expression on lymphocytes (left column) and CD8+ lymphocytes (right column) in AC, ATLL and healthy donor (HD). Horizontal bars indicate the mean percentage of PD-1-positive cells. The numbers below each patient represent the means ± s.d. (**c**) Percentage of PD-1 expression on human T-cell leukemia virus-1 (HTLV-1)-, cytomegalovirus (CMV)- and Epstein–Barr virus (EBV)-specific CD8+ lymphocytes and the percentage of tetramer+ cells in CD8+ lymphocytes in AC, ATLL and HD. Horizontal bars indicate the mean percentage of PD-1-positive cells. The numbers below each patient represent the means ± s.d. $^*P<0.001$; $^{**}P<0.01$; $^{***}P<0.05$ (Significant differences by Mann–Whitney *U*-test).